# Polysaccharide based nanoparticles for drug delivery applications

**Helene Jonassen**

Thesis submitted for the degree of Philosophiae Doctor

School of Pharmacy
Faculty of Mathematics and Natural Sciences
University of Oslo
2014

*Series of dissertations submitted to the*
*Faculty of Mathematics and Natural Sciences, University of Oslo*
*No. 1487*

ISSN 1501-7710



Cover: Inger Sandved Anfinsen.
Printed in Norway: AIT Oslo AS.

Produced in co-operation with Akademika Publishing.
The thesis is produced by Akademika Publishing merely in connection with the thesis defence. Kindly direct all inquiries regarding the thesis to the copyright holder or the unit which grants the doctorate.

*To my mother*

# Table of Contents

# Acknowledgements

*The work described in this thesis was carried out during the years 2008-2013 at the School of Pharmacy and the Department of Chemistry, University of Oslo, Norway.*

*First of all, I would like to thank my principal supervisor Professor Marianne Hiorth for all guidance and encouragement during these years, and for believing in me and supporting me during the more difficult periods. A special thank you goes to my co-supervisor Professor Anna-Lena Kjøniksen for great inspiration and tremendous amounts of help in completing this thesis. I would also like to thank my co-supervisors Professor Bo Nyström, for your enthusiasm and drive within the field of polymer chemistry, and Professor Sverre Arne Sande for introducing me to the field of statistical experimental design.*

*I am very grateful to my co-authors Alessandro Treves and Professor Gro Smistad for important contributions to the work on pectin nanoparticles, and to Tina R. Tuveng for technical assistance. A special thank you goes to Tove Larsen for technical guidance and assistance throughout all these years, and for always being willing to help! Thanks also go to Dr. Antje Hofgaard in the EM-lab, Department of Biosciences, University of Oslo for performing preliminary SEM-experiments on the chitosan nanoparticles.*

*I am indebted to Professor Jan Karlsen for arranging my master studies at the University of Sassari, Italy, and thereafter encouraging me to continue my PhD studies at the School of Pharmacy, University of Oslo.*

*I would also like to thank all present and previous members of the SiteDel research, which I have been so lucky to be a member of during these years. From the Department of Chemistry I would especially like to thank Ramón, Nodar and Loan for fruitful and fun meetings and discussions; Atoosa for your help in the very, very beginning of this work; and Kaizheng - hopefully I will be able to work with some of the polymers you have synthesized in the near future! Of the members from the School of Pharmacy and the Department of Biosciences I would especially like to thank Hilde-Gunn, Sanko, Teresa, Therese, Wai Lam, Wei and Lilia for all the enjoyable time we have shared together.*

*I would also like to thank all present and previous professors, technicians, post docs and students at the Department of Pharmacy, School of Pharmacy for the nice working environment. A special thank you goes to Marianne, Ravinder, Victoria and Kristine for being so nice office mates, and Milica for your enthusiasm and lovely cakes!*

*An additional thank you goes to Therese, Hilde-Gunn, Ravinder and Wai Lam for all the priceless discussions and fun we have had together!*

*Finally, I would like to thank my friends and family for always being there for me when I needed it the most. I am extremely grateful to my parents, Tom and Birgitta; this work could not have been completed without your endless love and support!*

*Oslo, February 2014*

*Helene Jonassen*

# Abstract

Nanoparticles are vastly studied drug delivery systems aiming at altering or improving the pharmacokinetics and pharmacodynamics of both low and high molecular weight drugs. Among the different materials used in the preparation of nanoparticulate drug delivery systems, polysaccharides offer several benefits, such as versatility, biodegradability and biocompatibility. Nanoparticles based on polysaccharides are thus promising drug delivery systems. In the formulation of new drug delivery systems, the understanding of the mechanisms and parameters affecting their properties is essential.

The considerations summarized above laid the grounds for this thesis with the overall aim of investigating parameters that could affect the preparation and physicochemical characteristics of nanoparticles based on the polysaccharides chitosan and pectin for potential applications in drug delivery. The main results obtained are reported in four papers that cover the development of a method for the estimation of the nanoparticle compactness, the preparation and characterization of nanoparticles based on chitosan or pectin, and the colloidal stability of the nanoparticles. Moreover, initial studies on the potential mucoadhesive properties of selected chitosan and pectin based nanoparticles are reported in this thesis summary.

The results presented demonstrate that both chitosan and pectin nanoparticles could be prepared by ionotropic gelation in the presence of sodium chloride, while chitosan microparticles and a macroscopic pectin network were formed in the absence of sodium chloride. The nanoparticle characteristics could easily be adjusted by changing the solvent salinity, the type and concentration of polysaccharide, and the crosslinker to polysaccharide ratio applied in the particle preparation. The main differences between the chitosan and the pectin nanoparticles were their positive and negative charge, respectively, and that the chitosan nanoparticles were generally smaller and more compact than the pectin nanoparticles. Both the chitosan and the pectin nanoparticles studied were mainly found to be colloidally stable after one week of storage. The chitosan nanoparticles interacted more strongly with mucin than the pectin nanoparticles *in vitro*, indicating a stronger ability to adhere to the body's protective mucus gel layer.

The findings in this thesis offer a decent platform for further studies on the applicability of polysaccharide based nanoparticles for drug delivery applications.

# List of papers

This thesis is based on the following papers, which are referred to in the text by their Roman numerals:

**I** H. Jonassen, A.-L. Kjøniksen
*Optical-scattering method for the determination of the local polymer concentration inside nanoparticles*
Physical Review E 84, 022401 (2011)

**II** H. Jonassen, A.-L. Kjøniksen, M. Hiorth
*Effects of ionic strength on the size and compactness of chitosan nanoparticles*
Colloid and Polymer Science 290, 919-929 (2012)

**III** H. Jonassen, A.-L. Kjøniksen, M. Hiorth
*Stability of chitosan nanoparticles cross-linked with tripolyphosphate*
Biomacromolecules 13, 3747-3756 (2012)

**IV** H. Jonassen, A. Treves, A.-L. Kjøniksen, G. Smistad, M. Hiorth
*Preparation of ionically cross-linked pectin nanoparticles in the presence of chlorides of divalent and monovalent cations*
Biomacromolecules 14, 3523–3531 (2013)

# List of abbreviations and symbols

| | |
|---|---|
| AFM | Atomic force microscopy |
| AM-pectin | Amidated, low-methoxylated pectin |
| CL | Crosslinker |
| $c_{NP}$ | Local polymer concentration inside the nanoparticles |
| DA | Degree of amidation |
| DDA | Degree of deacetylation |
| DDS | Drug delivery system |
| DE | Degree of esterification |
| DLS | Dynamic light scattering |
| FDA | United States Food and Drug Administration |
| LM-pectin | Low-methoxylated pectin |
| $M_n$ | Number average molecular weight |
| $M_w$ | Weight average molecular weight |
| $N_{agg}$ | Number of polymer chains inside the nanoparticles |
| NP | Nanoparticle |
| PDI | Polydispersity index (in DLS); a measure of the size polydispersity ($0 < PDI \leq 1$) |
| PEG | Polyethylene glycol |
| PS | Polysaccharide |
| q | Wave vector |
| $R_h$ | Hydrodynamic radius |
| TPP | Tripolyphosphate |
| Z-average | Cumulant mean (in DLS) |
| $\beta$ | Fitting parameter in the analysis of DLS data; gives a measure of the size polydispersity ($0 < \beta \leq 1$) |
| $\tau_f$ | Mean relaxation time |

# 1 Background

The term “drug delivery” refers to approaches or systems for administering a pharmaceutical active ingredient to achieve a therapeutic effect in humans or animals. These approaches or systems aim to improve treatment efficacy, safety and/or patient compliance and may involve the use of different medical devices, administration routes and drug formulations. Firstly, different medical devices can aid access to secluded parts of the human body, exemplified by the use of inhalators for improved drug delivery to the inner parts of the lungs. Secondly, different administration routes can be used for direct drug delivery to the site of action for local treatment, or for systemic drug delivery. The buccal administration route may for instance be used both for direct topical delivery of miconazole in the treatment of oral fungal infections [1, 2], and for systemic uptake of insulin in the treatment of Type I and Type II diabetes [3, 4]. Finally, different drug formulations or drug delivery systems (DDSs) may be used to modify the release profile, absorption, distribution, degradation or elimination of the active ingredient in the body to improve drug treatment.

Conventional DDSs are associated with a number of limitations when it comes to facilitating drug absorption, accessing the target site and timing the therapeutic effect [5, 6]. As further addressed below, nanoparticles offer new possibilities in the search for the “ideal” DDS; a system that is able to deliver the correct amount of drug to the desired site of action, at the correct rate and time, without any undesirable side-effects.

Polysaccharides are commonly used materials in the design of DDSs because they are generally regarded as biocompatible and biodegradable, and can possess other desired properties, such as the ability to adhere to the body’s mucosal linings. *Polysaccharide based nanoparticles* may hold the positive features of both nanoparticles and polysaccharides, and are suitable for both parenteral and mucosal administration of drugs [7-11].

The work presented in this thesis is an initiating study on nanoparticles based on the mucoadhesive polysaccharides chitosan and pectin for potential use as DDSs for mucosal administration. The work has particularly aimed at investigating the challenges connected to preparation of ionically crosslinked nanoparticles at relatively high polysaccharide concentrations and the estimation of the nanoparticle compactness.

# 2 Introduction

## 2.1 Nanoparticles in drug delivery

### 2.1.1 Nanoparticles as drug delivery systems

Nanoparticles can be defined as particles of various shapes having a size in the range 1 to 1000 nm. They can be comprised of both inorganic and organic constituents. This work, however, will focus on nanoparticles build up by organic materials, such as lipids, proteins, synthetic polymers and polysaccharides, with emphasis on the latter. Nanoparticles can act as drug delivery systems, having the drug entrapped in the interior structure, adsorbed to the surface, or covalently attached to the precursor materials [6, 11]. Since nanoparticles fall into the size range of macromolecular structures and proteins found inside living cells, they may take advantage of existing cellular machinery to deliver drugs [12].

One fundamental property of nanoparticles renders them different from their bulk materials, and that is the large surface-to-volume ratio [13]. This property may be exploited in formulation of hydrophobic drugs, for which an increase in surface area will increase the drug dissolution rate and enhance absorption [14]. The nanoparticles can also be taken up directly by cells in the mucosa through endocytosis [15, 16]. The composition of the nanoparticles may further enhance drug permeation and absorption, for instance by transiently opening tight junctions to facilitate paracellular drug or particle absorption [17]. In a study of solid-lipid-nanoparticles loaded with the biopharmaceutical classification system Class II drug cyclosporine A, a significant improvement in systemic drug levels was found if compared to drug nanocrystals after oral administration in pigs [18, 19]. This illustrates both the effect of the nanoparticle size and the composition on the bioavailability of the hydrophobic drug.

Certain pharmaceuticals such as proteins and peptides are easily degraded when administered orally and are often rapidly eliminated after intravenous injection [20, 21]. The incorporation of such pharmaceuticals in nanoparticles has therefore been exploited to protect them against premature physiological degradation and elimination [8, 16]. Cui et al. found for instance that PLGA (poly(D,L-lactide-co-glycolide)) nanoparticles containing hypromellose phthalate can protect insulin from the gastrointestinal environment, illustrated

by significantly reduced serum glucose levels after oral administration in rats, if compared with insulin solution [22].

Several physicochemical parameters may influence the biodistribution of nanoparticles after administration [23]. The penetration of nanoparticles through the protective gel layer covering the body's mucosal linings is for instance dependent on the size and surface characteristics [24, 25]. Studies have shown that nanoparticles smaller than approximately 200 nm can effectively diffuse through this gel layer, and that polystyrene nanoparticles coated with the uncharged hydrophilic polymer polyethylene glycol (PEG) penetrate more easily than uncoated polystyrene nanoparticles [26-28] .

Similar effects of size and surface characteristics have been found for the in vivo distribution and circulation of nanoparticles after intravenous injection. Coating the nanoparticles with PEG can for instance reduce the degree of opsonisation and clearance of the nanoparticles through the reticuloendothelial system in the liver, spleen and bone marrow, leading to longer circulation times and possibly enhanced deposition at the desired site [29, 30]. Rigid, spherical particles with a size of 100-200 nm are usually considered having the highest potential for prolonged circulation, as they are sufficiently large to avoid uptake in the liver and sufficiently small to avoid filtration in the spleen [29]. However, deformable soft nanoparticles of larger sizes may exhibit similar potentials [29]. Nanoparticles in the size range 100-200 nm are also attractive for passive targeting to tumors through the enhanced permeability and retention effect [30].

The surface of the nanoparticles can also be modified with ligands for targeted delivery, for example by incorporation of folate to target human cancer cells with an over-expression of folate receptors [12, 29]. There is also increasing interest in stimuli-responsive nanoparticles that can target or release the drug at a desired site or time upon exposure to various stimuli, such as physiological changes in pH or an externally applied magnetic field [13, 31, 32].

As shortly commented above, the fate of the nanoparticles in the human body is highly dependent on the physicochemical properties size, surface characteristics and deformability/compactness. These properties may also affect other important factors, such as the drug release profile [33-35] and the toxicity profile of the delivery system. It has for instance been reported that cationic nanoparticles can cause hemolysis and blood clotting,

while neutral and anionic nanoparticles are rather nontoxic [36]. The toxicity profile of the DDS is also linked to the properties of the precursor materials themselves [36]. The precursor materials and their possible degradation products should hence be biocompatible, and preferably biodegradable or able to be eliminated from the body to avoid accumulation and possible long-term toxicity. The size, charge and compactness of the nanoparticles also affect the colloidal stability in suspension [37-39], which can be of importance in the development of a final drug product suitable for commercialization.

### 2.1.2 Nanoparticles and mucosal administration

Much effort has been put into developing nanoparticles for the mucosal administration of drugs (e.g., by the oral, buccal and nasal administration routes), aiming for either enhanced systemic uptake or improved effect locally. These mucosal routes can be advantageous as they are less invasive than parenteral routes and do not require the production of sterile DDSs. However, these routes have a natural degrading and protective function which complicates the drug formulation development.

#### *2.1.2.1 The mucus barrier*

The mucosal epithelial linings in the body consist of tightly bound cells and are covered with a mucus gel layer for protection against the external environment. This protective layer is mainly composed of crosslinked and entangled mucin fibers forming a viscoelastic hydrogel consisting of typically 90-98% water [24, 25]. The pore size of the mucus network depends on the mucosal site and disease state, and can be in the range 50-1800 nm [40]. The mucus gel also contains other proteins, enzymes, antibodies, carbohydrates, lipids, salts, bacteria, cells and cellular debris, and is continuously cleared and replaced by the body [24]. The protective character of the mucus layer makes a natural barrier for drug penetration to the underlying cells for local therapeutic effects or systemic absorption. Therefore, DDSs that are able to either penetrate into or adhere to the mucus are widely studied for prolonging the retention time of the drug in close proximity to the site of action or absorption. Prolonged retention time may lead to a sustained drug delivery and reduced dosage frequency, and possibly improve patient compliance. A schematic representation of possible interactions between DDSs and the mucus layer is given in Figure 2.1. The figure illustrates the possibilities of interaction by polymer entanglements between polymer chains in the DDS and the mucin fibers, and the penetration of nanoparticles through the pores of the mucus gel network. More specific interactions between the DDS and the mucin fibers

may also contribute to the mucoadhesion, such as hydrophobic associations, electrostatic interactions and covalent bonds [24, 25].

The penetration of nanoparticles through the protective mucus layer is dependent on the particle size: it must be sufficiently small so that the particles can diffuse through the pores in the mucus mesh. Due to specific interactions with the mucus, conventional mucoadhesive nanoparticles generally penetrate the upper mucus layer only and do not easily reach the underlying epithelia [24, 25, 27, 28, 41]. A more novel approach to improve drug delivery at mucosal sites is to overcome the mucosal barrier by preparing mucus-inert nanoparticles that mimic the surface properties of viruses capable of diffusing in mucus as fast as in water [24, 25]. Hence, coating nanoparticles with uncharged and hydrophilic PEG of low-molecular weight has been found to increase the extent of mucus penetration with respect to uncoated hydrophobic nanoparticles [26, 27].

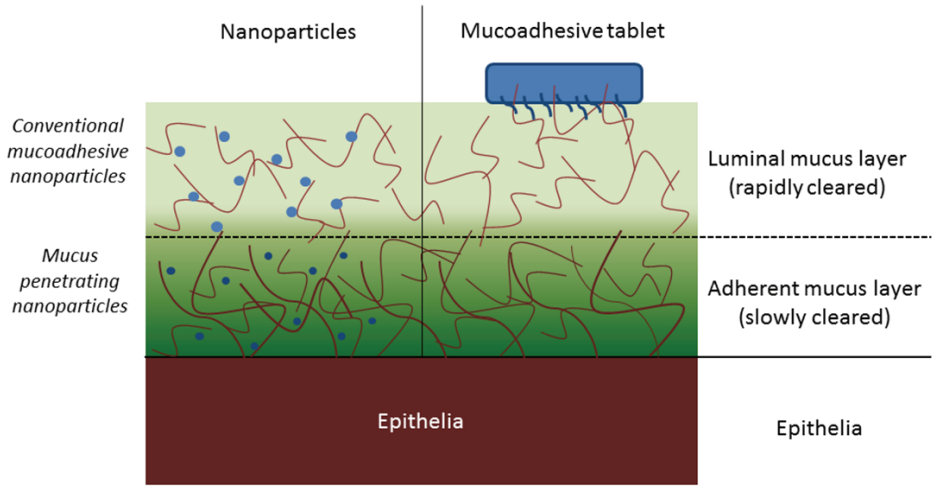


*Figure 2.1 – Schematic representation of the interaction of DDSs with the mucus layer. Upper left: mucoadhesive nanoparticles penetrating into the luminal mucus layer and sticking to the mucin fibers through hydrophobic associations or electrostatic interactions. Lower left: mucus-inert nanoparticles penetrating to the more stagnant mucus layer. Upper right: a mucoadhesive tablet sticking to the surface of the mucus layer. [25]*

To summarize, the potential advantages of nanoparticulate systems for improved delivery of drugs include 1) sustained maintenance of drug concentrations within the therapeutic window, 2) facilitation of administration of easily degradable agents, such as peptides and proteins, 3) decreased dosage frequency and possibly less invasive dosing, promoting patient compliance, 4) reduction of harmful side effects due to targeted delivery to a particular cell type or tissue, and 5) reduced manufacturing costs due to a reduction in the amount of drug needed or reduced microbiological requirements of the DDS [42]. These advantages must of course be balanced against 1) accumulation and toxicity of the materials or their degradation products, 2) unwanted rapid or burst release of the drug from the DDS, 3) increased discomfort of the DDS, and 4) expense of the DDS due to sophisticated manufacturing procedures or expensive materials [42].

## 2.2 Polysaccharide based nanoparticles for mucosal administration

### 2.2.1 Polysaccharides

Polysaccharides are linear or branched long-chained molecules composed of repeating sugar units adjoined by glycosidic bonds. They are highly abundant in nature and generally have low processing costs [11]. They can be of algal, plant, microbial or animal origin, and are widely used in formulation of both conventional and novel DDSs. Common examples of polysaccharides used in drug delivery are alginate, chitosan, hyaluronic acid, pectin and cellulose derivatives, such as hydroxyethyl cellulose and carboxymethylcellulose. Polysaccharides come in a wide range of molecular weights and chemical compositions, and can be divided into polyelectrolytes or non-polyelectrolytes, depending on the presence of ionizable functional groups. Due to a large number of reactive groups, most typically hydroxyl groups, they can easily be modified chemically and biochemically. This feature can be exploited in drug delivery, e.g., by conjugating drugs to the polysaccharides for sustained release, or by attaching ligands for targeting to a desired site.

Polysaccharides are hydrophilic in nature and may form macroscopic hydrogels at sufficiently high concentrations (above the overlap concentration) in the presence of cross-linkers or other substances inducing polymer-polymer interactions [7, 43]. The conformation of the polysaccharides in solution and the gelling properties are dependent on the balance between solvent-solute, solute-solute and solvent-solvent interactions, and is thus usually dependent on the solvent properties and the presence of co-solutes.

Polysaccharides are generally regarded as biocompatible, biodegradable and non-immunogenic, and hence safe materials for drug delivery. However, some conflicting results have been reported for the polysaccharide chitosan [44]. Another drawback of polysaccharides for drug delivery purposes is the potentially significant batch-to-batch variation due to their natural origin.

The degradation of polysaccharides in vivo is generally due to hydrolytic and enzymatic cleavage of the glycosidic bonds, and is highly dependent on the site of administration. Polysaccharides like pectin and chitosan are for instance enzymatically degraded by the bacteria in the colon, but to a small extent in the small intestine [17, 45, 46]. Hence, DDSs based on chitosan and pectin for possible drug targeting to the colon have been investigated [46-49]. Furthermore, polysaccharides, such as hyaluronic acid can be used for active targeting to cells expressing carbohydrate-binding cell-surface receptors [10, 50]. Several polysaccharides, like alginate and chitosan also possess mucoadhesive properties that can be exploited in mucosal delivery of drugs [51].

### 2.2.2 Preparation of polysaccharide based nanoparticles

Polysaccharide based nanoparticles can be prepared by different preparation methods, which can be divided into four categories: (1) covalent crosslinking, (2) ionic crosslinking, (3) polyelectrolyte complexation, and (4) self-assembly [11]. The different methods are briefly introduced below. The drug can either be physically entrapped during nanoparticle formation, covalently attached to the precursor materials, or absorbed or adsorbed to the nanoparticles post-preparation. Nanoparticles are often unstable in suspension, and as a final step, the nanoparticles are therefore often freeze-dried (in the presence of a suitable cryoprotectant) to extend their shelf-life [52]. The nanoparticles can be resuspended in a proper medium before administration. Another approach for extending the shelf-life is spray-drying into a microparticulate powder [52], which can be suitable for direct administration by inhalation or compression into tablets.

Covalent crosslinking

Nanoparticle preparation by covalent crosslinking involves the introduction of covalent bonds between the polysaccharide chains. This enables preparation of relatively robust nanoparticles, but is often avoided due to possible undesired side-reactions with the active ingredient and the toxicity of the crosslinker agents employed [7, 53]. However,

biocompatible crosslinkers like natural di- and tricarboxylic acids have been used to prepare biodegradable chitosan nanoparticles by the aid of the water soluble condensation agent carbodiimide [11, 54]. The condensation reaction involves the carboxylic groups of the natural acids and the amine groups of chitosan.

Ionic crosslinking

Ionic crosslinking (also called ionotropic gelation) is usually considered more advantageous than covalent crosslinking due to milder conditions and simpler experimental procedures. Under appropriate experimental conditions (i.e., suitable pH and dilute concentrations of precursor materials), nanoparticles can be prepared by ionically crosslinking polyelectrolytes with multivalent ions of opposite charge [11, 52, 53]. Nanoparticles based on alginate can for instance be prepared by crosslinking the ionized carboxyl groups on the alginate chains with $Ca^{2+}$-ions in aqueous media [55]. The most widely studied nanoparticles prepared by this method are perhaps chitosan nanoparticles crosslinked with tripolyphosphate (TPP), which was first reported by Calvo et al. in 1997 [11, 56]. TPP is a generally recognized as safe (GRAS) substance by the Unites States Food and Drug Administration (FDA) [57] and is negatively charged over a wide pH range. It can thus electrostatically interact with the protonated and positively charged amine groups of chitosan to form nanogels or nanoparticles. The crosslinking process can also be accompanied by other secondary inter-chain interactions, such as hydrogen bonding between chitosan's hydroxyl groups [7]. Parameters that potentially affect preparation of nanoparticles by ionic crosslinking includes the ionic strength of the solvent [58], the type [11] and molecular weight [59, 60] of polysaccharide, the polysaccharide concentration [61, 62], the crosslinker to polysaccharide ratio [63, 64], the pH [65, 66], and the mixing conditions [67, 68]. Ionically crosslinked nanoparticles can be considered less robust than covalently crosslinked nanoparticles, due to differences in bond strength [69].

Polyelectrolyte complexation

Polysaccharides with a polyelectrolyte character can form complexes with oppositely charged polymers through intermolecular electrostatic interaction. Chitosan is widely used; being one of the few positively charged polysaccharides. Other polysaccharides require chemical modification with for example oligo- or polyamines to obtain extensive positive charge. A common example of polyelectrolyte complexation is the interaction of chitosan

with negatively charged alginate [11]. Chitosan can also form polyelectrolyte complexes directly with negatively charged macromolecular drugs, such as nucleic acids [10, 70]. The mechanism for particle formation involves non-covalent, electrostatic interactions, but nanoparticles prepared by this mechanism may be more robust than ionically crosslinked particles due to the large portion of the polysaccharides involved in the complex formation [7].

Self-assembly

Polysaccharides with an amphiphilic character can spontaneously form nanoparticles in the form of micelles or polymer aggregates in an aqueous environment. The micelle formation takes place at concentrations above the critical micellar concentration. The underlying mechanism consists of inter and intra molecular associations between hydrophobic parts on the polysaccharide chains to minimize the interfacial free energy [11]. The particles can exhibit a core-shell structure with a hydrophobic core and a hydrophilic shell. Polysaccharides are generally hydrophilic, but can naturally possess some hydrophobic parts or be hydrophobically modified to facilitate self-assembly. Chitosan has for instance been modified with the long-chained acid linolenic acid to increase the amphiphilic character of the polysaccharide [71]. There has been some debate of the suitability of such self-assembled nanoparticles for drug delivery purposes, due to the possible loss of particle integrity upon dilution after administration [72].

The nanoparticle preparation may also be a mixture of the different methods. Nanoparticles can for instance be prepared by covalent crosslinking and subsequently coated with a polysaccharide of opposite charge through polyelectrolyte complexation on the particle surface.

### 2.2.3 Polysaccharide based nanoparticles as drug delivery systems

This work focuses on the polysaccharides chitosan and pectin due to these materials' intrinsic mucoadhesive properties and their ability to form nanoparticles in the presence of oppositely charged multivalent ions. Moreover, the difference in polyelectrolyte character of chitosan (positive) and pectin (negative) can facilitate incorporation of both negatively and positively charged drugs, thus enhancing the versatility of the polysaccharide based nanoparticulate DDSs.

#### *2.2.3.1 Chitosan and chitosan based nanoparticles*

Chitosan is obtained by deacetylation of the naturally occurring polysaccharide chitin, a structural component in the exoskeleton of arthropods and in the cell wall of fungi and yeast [17]. The main commercial sources of chitin and chitosan are crab and shrimp shells. Chitosan is composed of β-1,4-linked glucosamine and N-acetyl-D-glucosamine units, and is mainly characterized by the amount of deacetylated units and by its molecular weight. The degree of deacetylation (DDA) usually ranges from 70 to 95%, while the molecular weight varies widely from 10 to 1000 kDa [73].

The $pK_a$ value of chitosan has been reported to be approximately 6.3−6.6, and is affected by the DDA [17, 74, 75]. Chitosan is thus readily soluble in an acidic environment due to protonation of the amine groups and exhibits a polyelectrolyte character in solution. The use of acidic solvents can be avoided by utilizing water soluble quaternized or salt derivatives of chitosan. Several other derivatives of chitosan have also been synthesized to modulate its physical and biochemical properties [17, 76]. Thermosensitive chitosan derivatives have for instance been prepared by grafting poly(N-isopropyl-acrylamide) onto the chitosan chains [77]. Chitosan can be depolymerized and thermally degraded by hydrolytic cleavage, and is enzymatically degraded in the human body by lysozyme and in the colon by bacterial enzymes [17, 78].

Chitosan is generally regarded as biocompatible and biodegradable, exhibiting low cytotoxicity [17, 79]. Hence, chitosan is a suitable material for DDSs, but it is far from being an inert excipient. It may give an immunogenic response and has, among more, been found to exhibit antibacterial, antifungal, antioxidant and anticancer activity [53, 79-81]. Moreover, chitosan has mucoadhesive properties and the ability to transiently open tight-junctions to facilitate paracellular uptake of drugs [17, 76]. Chitosan is highly suitable for the delivery of negatively charged macromolecular drugs through mucosal administration routes. This is not only due to the possibility of drug encapsulation by electrostatic interactions between the positively charged chitosan and the negatively charged drugs, but also due to chitosan's ability to adhere to mucus and transiently opening tight-junctions.

Chitosan based nanoparticles are perhaps the most widely studied polysaccharide nanoparticles. They have been studied for delivery of both low and high molecular weight drugs at various administration routes [53, 70, 82]. For instance, Wang et al. studied the potential of using nanoparticles composed of the chitosan derivative chitosan-N-acetyl-L-

cysteine (chitosan-NAC) for systemic administration of insulin through the nasal route. They found that intranasal administration of chitosan-NAC nanoparticles in rats enhanced the absorption of insulin compared with unmodified chitosan nanoparticles and insulin solution [83].

In a study aiming at direct nose-to-brain targeting of estradiol, Wang et al. found that estradiol-loaded chitosan nanoparticles prepared by ionotropic gelation with TPP resulted in significantly increased drug levels in the cerebrospinal fluid after nasal administration if compared to intravenously administered nanoparticles [84]. Moreover, metronidazole containing chitosan nanoparticles for colon-specific delivery was evaluated in vitro by Elzatahry and Mohy Eldin and were found to exhibit excellent mucoadhesive properties and the ability to control the drug release over a period of 12 hours [85].

The versatility and positive charge of chitosan nanoparticles render them a natural choice in studies on polysaccharide based nanoparticles for potential use as DDSs for mucosal administration.

#### *2.2.3.2 Pectin and pectin based nanoparticles*

Pectin is a class of complex polysaccharides found in the cell wall of higher plants, and is widely used in the food industry as gelling and thickening agents. Pectins have a very complex and heterogeneous structure and consist primarily of homogalacturonan regions composed of repeating alpha-1,4-D-galacturonic acid units [47, 86, 87]. These so-called "smooth" regions are attached to "hairy regions" built up by alternating 1,2-linked alpha-D-galactose and alpha-L-rhamnose units. The hairy regions are highly branched with neutral arabinan, galactan and arabinogalactan side chains. Pectins are generally divided into two main categories, depending on the degree of methylesterified carboxyl groups (DE): high-methoxylated pectin (HM-pectin) with a DE above 50%; and low-methoxylated pectin (LM-pectin) with a DE below 50%. LM-pectin can also be modified by amidation [47], resulting in amidated low-methoxylated pectin (AM-pectin). The $pK_a$ value of the carboxyl groups of pectin is around 3.5 [86], and pectins are thus negatively charged at physiological pH (~7) and at most mucosal sites.

Pectins can be hydrolytically cleaved and degraded by bacterial enzymes in the colon [46, 87]. Pectins are generally considered biocompatible and biodegradable exhibiting low-toxicity, but as for chitosan, pectins are not completely inert excipients. They have for

instance been shown to exhibit mucoadhesive properties and the ability to target cancer cells expressing lectin receptors (which can bind to the galactose rich side chains of pectins) [10, 46, 47]. It should be noted that pectin was previously considered a poor mucoadhesive [88], however, more recent studies indicate the opposite [89-91].

Pectin nanoparticles are much less studied than chitosan nanoparticles. This may be linked to both the abundance of other negatively charged polysaccharides and the fact that pectin has a rather complex structure. However, a few promising studies can be mentioned. Opanasopit et al. found for instance that ionically crosslinked pectin nanoparticles have potential use as safe gene delivery vectors [64]: The plasmid DNA-loaded Ca-pectinate and Mg-pectinate nanoparticles prepared had the ability to transfect a human hepatoma cell line with low cytotoxicity. In another study by Sharma et al. [92], thiolated pectin nanoparticles where found to increase the ex vivo corneal permeation of the encapsulated drug, timolol maleate, if compared to a conventional solution dosage form. Moreover, Cheng and Lim showed that insulin can be incorporated into pectin nanoparticles crosslinked with calcium ions [93]. These particles were proposed for systemic delivery of insulin through the upper part of colon, which somewhat resembles the natural delivery route of physiological insulin [93].

Pectin based nanoparticles are promising DDSs as they, among more, may possess both mucoadhesive properties and targeting abilities. As opposed to chitosan nanoparticles, pectin based nanoparticles are negatively charged and less extensively studied in the literature. These considerations make pectin nanoparticles good candidates for studies on polysaccharide based nanoparticles for drug delivery applications.

# 3 Aim of the thesis

In the search for improved drug delivery systems, the understanding of the system's preparation and physicochemical characteristics is essential. Consequently, the overall aim of this thesis was to study the possibility to prepare nanoparticles from chitosan and pectin by ionotropic gelation and to investigate their physicochemical characteristics and properties.

The specific objectives of the studies were:

- To investigate parameters that can affect the particle preparation and important physicochemical properties, such as the particle size, charge and compactness
- To develop a method for the estimation of the compactness of the nanoparticles
- To investigate the stability of the nanoparticles in suspension
- To investigate the potential mucoadhesive properties of the nanoparticles

# 4 Summary of papers

## 4.1 Paper I

This paper describes a method based on the Mie theory for determining the local polymer concentration inside spherical nanoparticles ($c_{NP}$). The method can be used to obtain vital information about the compactness of nanoparticles in suspension, i.e., the degree of particle swelling. In addition, the method can be used to calculate the number density of the particles, the molecular weight of the particles, and (if the number average molecular weight, $M_n$, of the polymer is known) the aggregation number of polymer chains inside the nanoparticles ($N_{agg}$). The calculations are based on the relationship between the size of the nanoparticles and the turbidity of the sample. The method was experimentally tested on chitosan nanoparticles prepared by crosslinking chitosan with tripolyphosphate (TPP) in aqueous media (0.10 M NaCl). It was found, as expected, that the compactness of the particles increased with the crosslinking density (i.e., the TPP concentration).

## 4.2 Paper II

In this paper, several combinations of chitosan nanoparticles were prepared by ionotropic gelation of chitosan with TPP in aqueous media. The effects of the ionic strength of the solvent (0, 0.05 and 0.15 M NaCl) employed in the particle preparation on the average size and compactness of the particles were investigated. In addition, the effects of the chitosan chloride concentration (0.05 and 0.10%) and the crosslinker to polysaccharide ratio (5:95, 10:90, 15:85 and 20:80) on the particle characteristics were studied. The chitosan-TPP nanoparticles were characterized by dynamic light scattering, zeta potential, and turbidity measurements. The compactness of the nanoparticles was estimated by using the method reported in paper I.

All the investigated preparation parameters, i.e., the ionic strength of the solvent, the chitosan concentration and the TPP to chitosan ratio, affected the particle characteristics. If compared to particles prepared in pure water, smaller and more compact particles were formed in the presence of sodium chloride. It was also observed an increase in the average particle size with an increase in the chitosan concentration, however, only moderate changes in the average particle size were found with increasing TPP to chitosan ratios. The particle compactness increased with higher solvent salinity and TPP to chitosan ratios, while no

differences in the compactness of the particles prepared at low and high chitosan concentration were observed when a moderate amount of TPP was employed.

## 4.3 Paper III

In this paper, the physical stability of chitosan nanoparticles crosslinked with TPP was investigated over a period of one month. Special emphasis was placed on changes in the particle size and the particle compactness. The chitosan-TPP particles were prepared at different ionic strengths (0, 0.05 and 0.15 M NaCl), chitosan chloride concentrations (0.05 and 0.10%) and TPP to chitosan ratios (5:95, 10:90, 15:85 and 20:80). In the presence of monovalent salt, the positive zeta potential of the particles was reduced. In spite of this, the particles were more stable when prepared and stored under saline conditions compared to pure water. This could be attributed to the smaller particle sizes found in the presence of sodium chloride. Most of the particles prepared in saline solvents were stable with respect to changes in the size and the compactness of the particles. However, instability was observed at the highest crosslinker to polysaccharide ratios. Generally, a reduction in the zeta potential and an increase in the particle compactness were observed at increasing TPP to chitosan ratios (paper II). This combined with the size increase induced by a high concentration of chitosan, increased the aggregation and sedimentation tendency of the particles and reduced the colloidal stability of these particles.

## 4.4 Paper IV

In this paper, nanoparticles were prepared by ionotropic gelation of low-methoxylated (LM) and amidated low-methoxylated (AM) pectin with zinc chloride ($ZnCl_2$) in aqueous media. The samples were characterized by atomic force microscopy, dynamic light scattering, turbidimetry, zeta potential and pH measurements. Negatively charged pectin nanoparticles could be prepared at a pectin concentration of 0.07% and a $ZnCl_2$ to pectin ratio of 15:85 in the presence of sodium chloride (0.05 M), but not in pure water. Interestingly, particles in the nanometer size-range could also be prepared in the absence of the crosslinker $ZnCl_2$. The AM-pectin nanoparticles were much less polydisperse than the LM-pectin nanoparticles, and hence considered more promising as a potential drug delivery system.

Further studies were performed to investigate the colloidal stability and the effect of the pectin concentration on the size, charge and compactness of the AM-pectin nanoparticles. These studied showed that the self-associated AM-pectin nanoparticles (prepared in the

absence of $ZnCl_2$) were stable for one month of storage, while the crosslinked AM-pectin nanoparticles were stable for one week. This difference in colloidal stability could be attributed to the reduced absolute zeta potential values of the crosslinked nanoparticles. Increasing AM-pectin concentrations from 0.03 to 0.07% resulted in a size increase of the self-associated nanoparticles, but not of the crosslinked nanoparticles. This lack in size increase was connected with an increase in particle compactness of the crosslinked nanoparticles with increasing AM-pectin concentrations.

# 5 Experimental considerations

Experimental considerations and descriptions of the main materials and methods used in papers I-IV are given in this section. Further details can be found in the individual papers. The in vitro interaction studies between two selected nanoparticle formulations and mucin are, however, only described herein.

## 5.1 Materials

Both chitosan and pectin possess mucoadhesive properties and the ability to gel in the presence of multivalent ions of opposite charge. However, chitosan is positively charged (below pH ~6.5) and a rather well-studied polysaccharide for preparation of nanoparticles, while pectin is negatively charged (above pH ~3.5) and much less studied. These considerations formed the basis for the choice of pectin and chitosan for preparation of nanoparticles with potentially similar, yet different properties.

*Table 5.1 – Materials*
*$M_w$ = Weight average molecular weight; $M_n$ = Number average molecular weight; DDA = Degree of deacetylation; DE = Degree of esterification; DA = Degree of amidation; GalA = Galacturonic acid; Rha = Rhamnose*
** % of total carbohydrate content (data published by Smistad et. al [94])*
*# simplified structure, see [94]and section 2.2.3.2 for a more comprehensive description of the pectin structure*

| Polysaccharide | Specific properties | Molecular structure | Paper |
|---|---|---|---|
| Chitosan | Hydrochloride salt<br>$M_w = 3.07\times10^5$<br>$M_w/M_n = 2.7$<br>DDA = 83% | 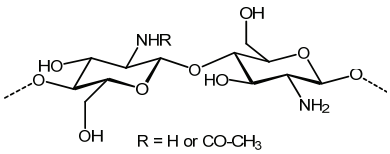 | **I, II, III** |
| LM-pectin | $M_w = 7.6\times10^4$<br>$M_w/M_n = 1.6$<br>DE = 35%<br>GalA = 86.8% , Rha = 4.4%* | 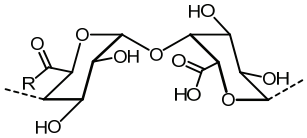 | **IV** |
| AM-pectin | $M_w = 9.6\times10^4$<br>$M_w/M_n = 1.2$<br>DE = 30% , DA = 19%<br>GalA = 86.3% , Rha = 3.3%* | LM-pectin: R = OH or O-CH3<br>AM-pectin: R = OH or O-CH3 or NH2<br># simplified structure | **IV** |
| **Crosslinker** | | | |
| Tripolyphosphate (TPP) | Sodium salt | 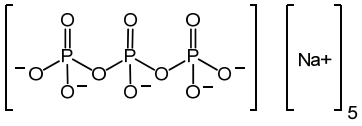 | **I, II, III** |
| Zinc chloride | Anhydrous | $ZnCl_2$ | **IV** |

An overview of the types of polysaccharides and crosslinkers used in the different papers are given in Table 5.1.

The hydrochloride salt of chitosan was chosen because it is embedded in the European Pharmacopeia and water soluble. Moreover, chitosan with a high DDA (83%) was used to ensure sufficient protonation and interaction with the anionic crosslinker. The crosslinker salt chosen for preparation of chitosan nanoparticles was the pentasodium salt of tripolyphosphate, which is generally recognized as safe by the FDA [57].

Pectin with low DE was chosen since this type can easily gel in the presence of divalent cations [46, 95]. An amidated form of low-methoxylated pectin was also included to potentially adjust the properties of the nanoparticles prepared. Zinc ions have been applied as an alternative to calcium ions in the preparation of macroscopic pectin gels [91] and can also be used as an active ingredient, for instance in the treatment of bad breath [96]. The crosslinker chosen for the preparation of ionically crosslinked pectin nanoparticles was therefore zinc chloride.

*Table 5.2 – Overview of parameters used in the particle preparation*
*PS = Polysaccharide; CL = Crosslinker; NP = Nanoparticle ; TPP = Tripolyphosphate*

| Paper | Type of PS | Type of CL | Solvent | PS conc. (%, $^{w}/_{w}$) | PS to CL ratio (w:w) | Batch size of NP dispersion (g) | Total stirring time (min) |
|---|---|---|---|---|---|---|---|
| **I** | Chitosan | TPP | 0.10 M NaCl | 0.10 | 5:95 , 9:91<br>13:87 , 17:83<br>20:80 , 23:77 | 30 | 5 |
| **II** | Chitosan | TPP | $H_2O$<br>0.05 M NaCl<br>0.15 M NaCl | 0.05<br>0.10 | 0:100<br>5:95 , 10:90<br>15:85 , 20:80 | 75 | 10 |
| **III** | Chitosan | TPP | $H_2O$<br>0.05 M NaCl<br>0.15 M NaCl | 0.05<br>0.10 | 0:100<br>5:95 , 10:90<br>15:85 , 20:80 | 75 | 10 |
| **IV** | LM-pectin | $ZnCl_2$ | $H_2O$<br>0.05 M NaCl | 0.07 | 0:100<br>15:85 | 75 | 10 |
| **IV** | AM-pectin | $ZnCl_2$ | $H_2O$<br>0.05 M NaCl | 0.03<br>0.05<br>0.07<br>0.09 | 0:100<br>15:85 | 75 | 10 |

## 5.2 Methods

### 5.2.1 Particle preparation by ionotropic gelation

Ionotropic gelation by crosslinking charged polymer chains with oppositely charged multivalent ions is a simple and fast technique for the preparation of nanoparticle dispersions. In this thesis, the ionotropic gelation was performed by adding a fixed amount of crosslinker solution drop-wise to a fixed amount of dilute polysaccharide solution under magnetic stirring (see illustration in Figure 5.1). The speed of crosslinker addition (pump speed = 25 rpm), the size of the magnetic bar (20 × 6 mm) and the magnetic stirring speed (550 rpm) were kept constant in all papers. The particles were prepared at different polysaccharide concentrations in water with varying amounts of sodium chloride, and at different crosslinker to polysaccharide ratios, as given in Table 5.2. The pectin nanoparticles were only prepared at a sodium chloride concentration of 0.05 M because the preliminary results (performed on LM-pectin) at high concentrations (0.15 M) were unsatisfactory. The batch size (and the vial size) might affect the stirring conditions and thus also the properties of the nanoparticles. The batch size in papers II-IV was therefore kept constant to better compare the different particles prepared, and accordingly the amounts of crosslinker solution (15 g) and polysaccharide solution (60 g) prior to mixing were also kept constant. Borosilicate glass vials for injection were used in all papers (50 mL in paper I; 100 mL in papers II-IV). It should be noted that the tubing used in paper IV had a wider inner diameter, resulting in a faster addition of the crosslinker solution (approximately 8 g/min vs. 3.5 g/min in papers I-III), which might affect the crosslinking process.

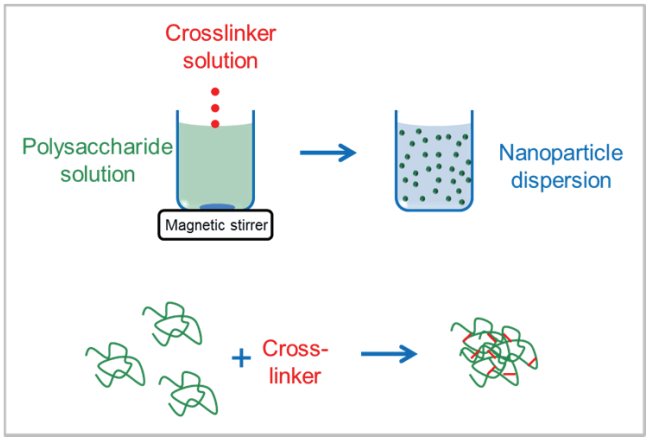


*Figure 5.1 – Schematic illustration of the particle preparation.*

### 5.2.2 Dynamic light scattering

Dynamic light scattering is a non-invasive and well-established technique for measuring size and size distributions of particles in the submicron region, and can also be used to study the behavior of complex fluids, such as concentrated polymer solutions. A schematic illustration of the passage of light in DLS experiments is given in Figure 5.2.

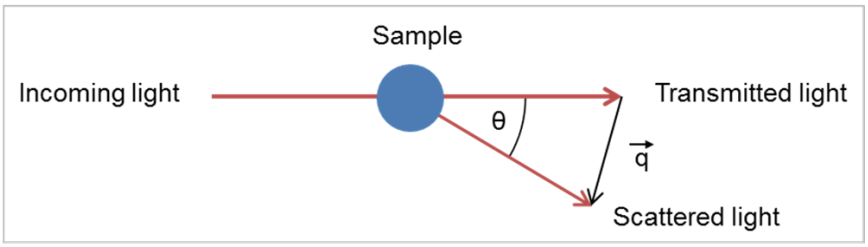


*Figure 5.2 – Schematic illustration of the passage of light in DLS experiments.*

The principle of DLS size measurements relies on the fact that the Brownian motion of suspended particles will cause time dependent fluctuations in the intensity of the scattered light. These fluctuations are recorded at different scattering angles (θ) or wave vectors (q) and expressed in terms of autocorrelation functions. The wave vector is defined as $q=4\pi n\sin(\theta/2)/\lambda_L$, where $\lambda_L$ is the wavelength of the incident light in vacuum, θ is the scattering angle, and $n$ is the refractive index of the sample. Assuming that the scattering field obeys Gaussian statistics, the experimentally measured homodyne intensity autocorrelation function $g^2(q,t)$ in DLS measurements is directly linked to the theoretically amenable first-order electric field autocorrelation function, $g^1(t)$, through the Siegert relationship [97]: $g^2(q,t) = 1 + B\left|g^1(t)\right|^2$, where B (≤ 1) is an instrumental parameter and t is the time. The mean relaxation time ($\tau_f$) and the mutual diffusion coefficient (D) of the particles can be derived from the autocorrelation functions. Assuming that the particles are compact spheres, the mean hydrodynamic radius, $R_h$, of the particles can be calculated from D using the Stokes-Einstein relationship:

$$R_h = \frac{k_B T}{6\pi\eta D}$$

where $k_B$ is the Boltzmann constant, T is the absolute temperature, and η is the viscosity of the solvent at the given temperature.

In this thesis, two different light scattering instruments were used: an ALV/CGS-8F Compact Goniometer System from ALV-GmbH, Germany (papers I-IV), and a Zetasizer Nano NZ from Malvern Instruments Ltd., UK (paper IV). The ALV-goniometer is equipped with a 22 mW He-Ne-laser, operating at a wavelength of 632.8. The intensity of the scattered light can be measured at 8 different angles simultaneously, and any angular dependency of the calculated $R_h$ can thus easily be checked. The Zetasizer Nano NZ is equipped with a 4 mW He-Ne-laser (operating at a wavelength of 632.8) and uses non-invasive back-scattering detection at a fixed angle of 173°. The fixed detection angle precludes the control of any angular dependency of the calculated $R_h$.

In papers I-IV, the $g^1(t)$ functions obtained from the ALV goniometer were fitted to a stretched exponential function $g^1(t) = \exp\left[-(t/\tau_{fe})^{\beta}\right]$, where $\tau_{fe}$ is an effective relaxation time and $\beta$ is a fitting parameter ($0 < \beta \leq 1$). The value of $\beta$ gives an indication of the distribution width of the relaxation times and thus the size distribution (monodisperse samples have a $\beta$ value close to 1). The mean relaxation time ($\tau_f$) was calculated through the following relationship: $\tau_f = \frac{\tau_{fe}}{\beta}\Gamma\frac{1}{\beta}$, where $\Gamma(1/\beta)$ is the gamma function. In all papers, the relaxation times were found to be diffusive ($\tau_f \sim q^{-2}$), and the mutual diffusion coefficients were thus obtained from the following expression: $D = 1/(\tau_f q^2)$. Finally, the apparent, mean $R_h$ of the particles was calculated using the Stokes-Einstein relationship given above. The average $R_h$ values reported were obtained by calculating the arithmetic mean of multiple measurements (n = 3-4) on the same batch.

In paper IV, the ALV goniometer was primarily used on representative samples to check the angular dependency of the $R_h$ and to confirm that $\tau_f \sim q^{-2}$. The $R_h$ and polydispersity index (PDI) values reported in paper IV were thus obtained from experiments performed on the Zetasizer Nano NZ. The general purpose fitting method in the Zetasizer software was chosen for the calculation of the mean $R_h$ values, since this fitting method gives values that are comparable to the ones obtained from experiments on the ALV goniometer [98]. The mean $R_h$ value of each batch was calculated from multiple measurements (n > 3) by the Zetasizer software. The average $R_h$ values reported were obtained by calculating the arithmetic mean of separate batches (n = 2-3). The PDI is a measure of the size distribution with values in the range 0 to 1. Monodisperse samples have a PDI value less than 0.1, while PDI values greater than 0.7 indicate a very broad size distribution.

### 5.2.3 Zeta potential measurements

The zeta potential is a common measure of the magnitude of the electrostatic charge of particles in dispersion, and is highly relevant in stability studies of nanoparticle suspensions. Generally, zeta potentials above an absolute value of 30 mV are considered necessary to ensure good colloidal stability [99-101].

Charged particles in aqueous dispersion are surrounded by ions in an electric double layer. This liquid double layer consists of an inner region (Stern layer) with relatively strongly bound counter-ions, and an outer region with less firmly associated ions. The zeta potential is the electric potential at the slipping plane (see Figure 5.3), i.e., at the surface of the stationary liquid double layer.

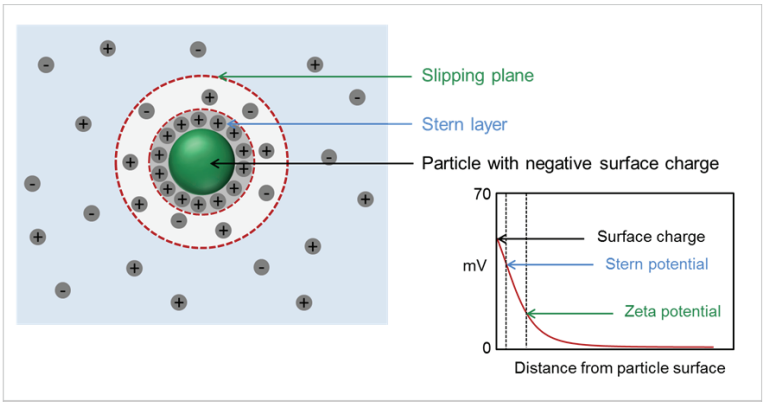


*Figure 5.3 – Schematic illustration of a negatively charged particle in aqueous media*

Zeta potential measurements on particle dispersions are commonly performed by electrophoresis, which is based on the migration of charged particles when exposed to an electric field. The velocity of the migrating particles can be measured by Laser Doppler velocimetry, in which the frequency shift or phase shift of an incident laser beam caused by the moving particles is used to calculate the electrophoretic mobility, $U_E$, of the particles. The zeta potential (ζ) can then be calculated from the Henry equation:

$$U_E = \frac{2\varepsilon\zeta}{3\eta} f(Ka)$$

where η and ε are the viscosity and the dielectric constant, respectively, of the solvent at a given temperature. The Smoluchowski approximation to Henry's function (f(Ka) = 1.5) was applied in all papers (II-IV).

In this thesis, two similar instruments measuring the zeta potential by electrophoresis and Laser Doppler velocimetry were used (both from Malvern Instruments Ltd., UK): Malvern Zetasizer 3000HSA (papers II and III) and Zetasizer Nano NZ (paper IV).

### 5.2.4 Turbidity measurements

Turbidity is a measure of a sample's ability to hinder the passage of light. Consequently, the turbidity of a nanoparticle dispersion is affected by the number and the size of the particles present, and by the difference in refractive index between the particles and the solvent. Turbidity measurements can be conducted by the means of a spectrophotometer. In contrast to DLS measurements, where the scattered light intensity is detected, it is the transmitted light intensity that is detected in turbidity measurements. The turbidity can be calculated using the following expression (Lambert-Beer's law):

$$\tau = -\frac{1}{L}\ln\left(\frac{I_t}{I_0}\right)$$

where L is the light path length in the sample cell, $I_t$ is the intensity of the light transmitted through the sample, and $I_0$ is the intensity of the light transmitted through the solvent.

In this thesis, a temperature controlled Helios Gamma spectrophotometer from Thermo Spectronic, UK, was used for the turbidity measurements.

### 5.2.5 Determination of the particle compactness

The determination of the compactness of nanoparticles in suspension, or the degree of particle swelling, can be difficult to perform experimentally. In paper I, a theoretical method was developed to overcome these difficulties. The method combines data from DLS and turbidity measurements to calculate the local polymer concentration inside nanoparticles, $c_{NP}$, which can be used as a measure of the particle compactness. Accordingly, increasing $c_{NP}$ values correspond to higher particle compactness.

The $c_{NP}$ can be calculated through the following expression (paper I):

$$\tau = \frac{3c_t}{2c_{NP}R_h}\left[1 - \frac{2}{wc_{NP}}\left(\sin(wc_{NP}) - \frac{1}{wc_{NP}}(1-\cos(wc_{NP}))\right)\right]$$

where $\tau$ is the turbidity of the nanoparticle suspension, $R_h$ is the hydrodynamic radius of the particles, $c_t$ is the total polymer concentration in suspension, and $w = \frac{4\pi R_h (dn/dc)}{\lambda_T \, n_0}$, where $n_0$ is the refractive index of the solvent, $\lambda_T$ is the wave length at which the turbidity measurements were performed, and dn/dc is the refractive index increment of the polymer. The method is developed for spherical, monodisperse particles, and the total polymer concentration that exists in the form of nanoparticles must be known. These considerations could be assumed for the crosslinked nanoparticles prepared in the presence of sodium chloride, since $\tau_f \sim q^{-2}$ indicated spherical particles, and since the relatively high crosslinker concentrations and ionic strength promoted polysaccharide aggregation and narrow size distributions (paper II and IV). It should be noted that the method is not suitable for the estimation of the $c_{NP}$ of core-shell nanoparticles with distinctly different refractive indices of the core and shell, since such particles will exhibit a more complex scattering profile.

### 5.2.6 Interaction studies with mucin

In order to evaluate the nanoparticles' potential mucoadhesive properties, an in vitro interaction test with mucin[1] was performed on two nanoparticle formulations, one made from chitosan and one made from AM-pectin. The nanoparticles chosen were prepared in 0.05 M NaCl at a crosslinker to polysaccharide ratio of 15:85 (w:w) and at a polysaccharide concentration of 0.05% (w/w).

The method reported by Klemetsrud et al. [98] was used, with small modifications. Shortly, 5 mL of a 0.10% (w/w) solution of mucin in 0.05 M NaCl was added drop-wise to 10 mL of nanoparticle suspension under magnetic stirring. The resultant mixtures were evaluated visually and, if suitable, by DLS, turbidity and zeta potential measurements the following day. Controls were prepared by mixing the mucin solution and the nanoparticle suspensions with 10 and 5 mL of 0.05 M NaCl, respectively.

[1] Water soluble mucin from bovine submaxillary glands, type I-S, used as received (Sigma-Aldrich, USA).

# 6 Main results and discussion

## 6.1 Preparation of nanoparticles

The first objective of this study was to investigate parameters affecting the preparation of nanoparticles based on the polysaccharides chitosan and pectin. The nanoparticle preparation method chosen was ionotropic gelation, which is considered a simple and mild technique suitable for scaling up [53, 68]. To assure formation of nanoparticles, the ionotropic gelation should be performed at dilute polysaccharide concentrations [52], avoiding extensive polymer chain overlap and hence formation of larger particles or a macroscopic gel. The conformation and the extent of chain overlap of polysaccharides in solution are dependent on the type and concentration of polysaccharide, the solvent properties and the thermodynamic conditions. For the polyelectrolytes chitosan and pectin, the conformation in aqueous media is naturally dependent on their $pK_a$ values and the pH. At a pH supporting ionization of the amine and carboxyl groups on chitosan and pectin, respectively, the polysaccharide chains will have an extended conformation in pure water due to charge repulsion between the ionized groups [87, 102].

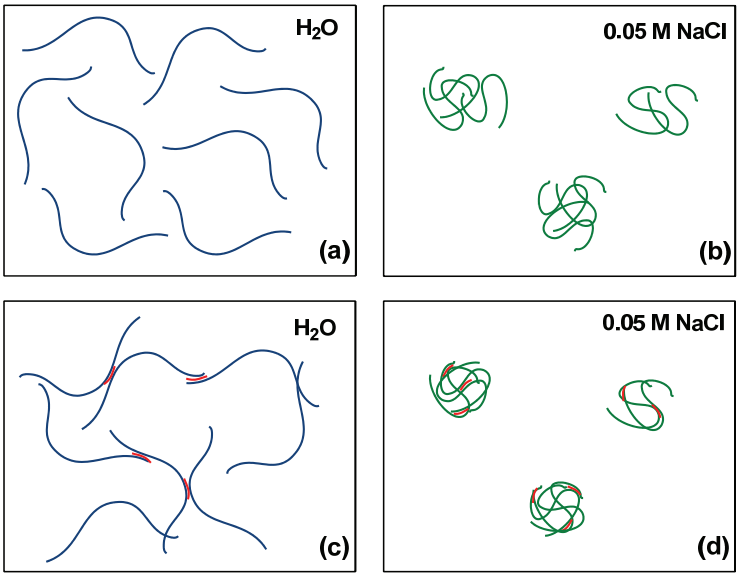


*Figure 6.1 – Proposed conformation of charged polysaccharide chains in (a) pure water, and (b) 0.05 M NaCl, and crosslinked polysaccharide chains in (c) water and (d) 0.05 M NaCl. Junction zones are given in red.*

The easiest way to minimize the overlap between the polysaccharide chains is to reduce the polysaccharide concentration below the overlap concentration. The major drawback of doing this is that the total batch volume will increase with respect to the amount of particles formed. This may pose problems considering both the sensitivity limitations in the characterization techniques and an eventual up-scale of the particle preparation. This is especially the case if working with charged polyelectrolytes in pure water, having an extended conformation in solution.

Another way of reducing the extent of overlap of the polysaccharide chains is to add monovalent salt. Monovalent salts present in sufficient amounts can reduce the electrostatic repulsion between the charged groups, thus promoting contraction of the polysaccharide chains and reduced chain overlap [103]. In this way, a smaller total batch volume will be required to obtain the same amount of nanoparticles. Furthermore, if the particles are prepared at an ionic strength similar to that of physiological fluids they are more likely to maintain their integrity when administered to the patient. Increasing the ionic strength during the particle preparation can, however, be a drawback in cases where a significant ionic interaction between the carrier and the encapsulated substances is required during the particle preparation. A schematic representation of the proposed conformation of charged polysaccharide chains in pure water and in the presence of 0.05 M NaCl is given in Figure 6.1, along with the proposed effects on the ionic crosslinking process.

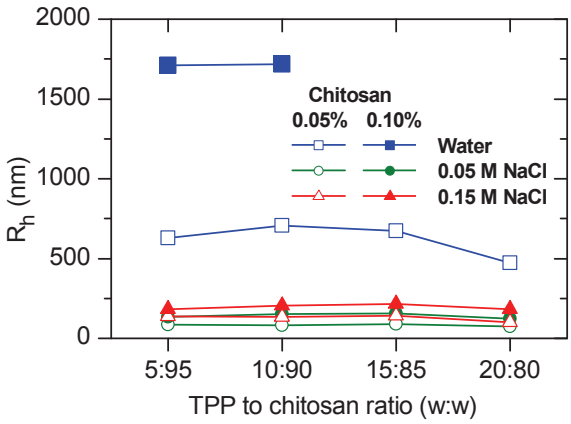


*Figure 6.2 – The average $R_h$ of chitosan nanoparticles one day after particle preparation. Connection lines between the symbols are given in order to guide the eyes. Samples in which particle sedimentation was observed are omitted from the figure. The standard deviations of $R_h$ are equal to or smaller than the size of the symbols.*

In paper II and IV, the preparation of ionically crosslinked chitosan (paper II) and pectin (paper IV) nanoparticles was investigated in detail. With the effects on the polysaccharide conformation kept in mind, it was initially hypothesized that the nanoparticle preparation would be greatly affected by the ionic strength of the solvent. Additionally, two preparation parameters that were both easily adjustable and likely to affect the particle characteristics were investigated: the polysaccharide concentration [61, 62, 67] and the crosslinker to polysaccharide ratio [60, 62, 64].

Preliminary experiments indicated that the formation of pectin nanoparticles was more sensitive to changes in the preparation parameters than the chitosan nanoparticles. Accordingly, different experimental set-ups for the preparation of the chitosan and the pectin nanoparticles were chosen. The main differences in the preparation parameters were *the sodium chloride concentration* and *the crosslinker to polysaccharide ratio*, which were varied in the paper on chitosan nanoparticles (paper II), but kept constant in the paper on pectin nanoparticles (paper IV). Moreover, the effect of chitosan concentration was investigated in paper II, while the pectin concentration was (initially) kept constant in paper IV.

It was found that chitosan particles in the nanometer size range could be prepared in the presence of sodium chloride (see Figure 6.2). In pure water, however, the chitosan particles formed were mostly microparticles, and at high chitosan and crosslinker concentrations large aggregates that immediately sedimented were formed rather than the desired

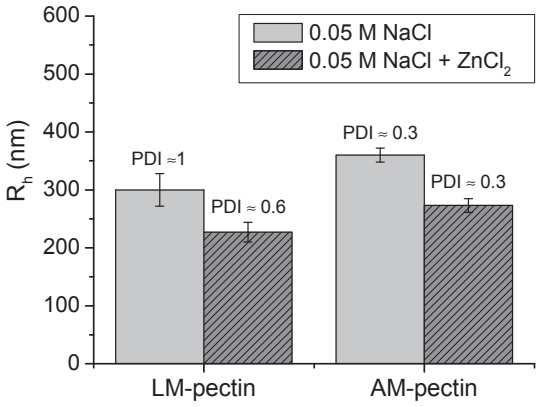


*Figure 6.3 – The average $R_h$ of self-associated and crosslinked pectin nanoparticles at a concentration of 0.07% pectin one day after particle preparation. The PDI values are also given.*

nanoparticles. In the study on pectin particles (paper IV), a partially crosslinked, macroscopic polymer network was formed in pure water, while in the presence of sodium chloride both non-crosslinked and crosslinked nanoparticles were formed (see Figure 6.3). The self-association of pectin into nanoparticles in the presence of monovalent anions and cations can be seen in the atomic force microscopy (AFM) images given in Figure 6.4. The self-association can be due to promotion of hydrogen bonding or hydrophobic associations [87, 95] at higher ionic strengths.

From the studies performed in paper II and IV it can be concluded that nanoparticles based on chitosan and pectin can be prepared by ionotropic gelation in the presence of sodium chloride, which assumingly reduce the extent of polysaccharide chain overlap and promotes formation of small crosslinked nanoparticles rather than large clusters or a macroscopic polymer network. A more comprehensive presentation of the effects of the preparation parameters on the physicochemical characteristics of the nanoparticles is given in the following section.

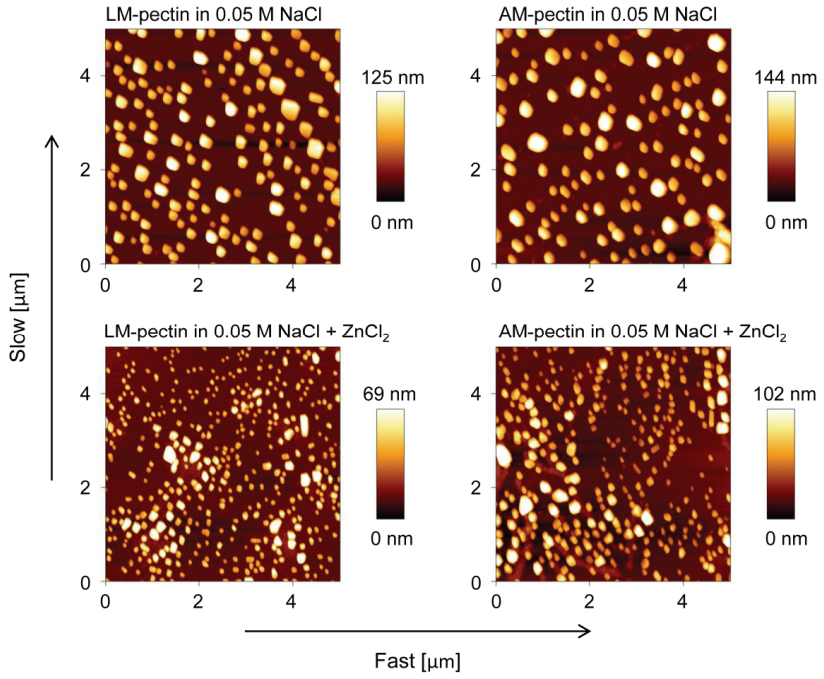


*Figure 6.4 – AFM images of dried LM- and AM-pectin samples in 0.05 M NaCl, at a pectin concentration of 0.07%, with and without $ZnCl_2$. The images were obtained by scanning in lines (fast scanning direction) from the bottom to the top (slow scanning direction), as indicated by the arrows.*

## 6.2 Particle characteristics

One of the major objectives in this thesis was to characterize the nanoparticles' physicochemical properties, with special emphasis on particle size, charge and compactness. These properties may influence the nanoparticles' suitability as a drug delivery system, as already mentioned in the Introduction section. The particles prepared in this thesis were composed of two different polysaccharides and varied in size, charge and compactness, thus giving a decent platform for further studies on their suitability as drug delivery systems. The main observations and differences found for the nanoparticles prepared are presented in the following three sub-sections. The results presented were obtained one day after particle preparation, unless otherwise described.

### 6.2.1 Size and size distribution

Preliminary experiments indicated that the particle preparation of pectin nanoparticles was rather sensitive to the ionic strength and the crosslinker concentration. Therefore, the pectin nanoparticles were prepared at fixed sodium chloride and crosslinker concentrations. The chitosan nanoparticles could, however, be prepared in a broad range of sodium chloride concentrations and crosslinker to chitosan ratios.

In Figure 6.2 (page 32) one can clearly observe that the presence of monovalent salt reduced the size of the chitosan particles from micrometers to nanometers in diameter. As discussed in section 6.1, this can be explained by a reduction in the electrostatic repulsion between the polymer chains leading to a contracted conformation in solution prior to crosslinking. As can be seen in Figure 6.5, the size of the chitosan nanoparticles was not significantly affected by an increase in the sodium chloride concentration up to 0.10 M. However, upon further increase to an isotonic concentration of 0.15 M NaCl the particle size increased slightly. It has previously been shown that an increase in the ionic strength of the media favors inter-chain association of chitosan molecules in solution [104], which may explain the observed size increase. The observed raise in the number of polymer chains inside the nanoparticles ($N_{agg}$) with an increase in the sodium chloride concentration (paper II) supports this explanation. It should be noted that the batch size of the nanoparticle dispersions prepared at 0.10 M NaCl was smaller than the ones prepared at 0.05 and 0.15 M NaCl, which may have affected the particle characteristics slightly. A reduced batch size, but constant stirring conditions, induces higher sheer stress on the system which can both reduce and increase the aggregation tendency of polymers during the crosslinking process

[105, 106], and it is hence difficult to conclude if the reduction in batch size can explain the slightly smaller sizes observed.

The β values obtained from the DLS measurements give an indication of the distribution width of the relaxation times and thus the particle size distributions (monodisperse samples have a β value close to 1). The β values obtained for the particles studied in paper II were significantly higher at 0.15 M NaCl if compared to 0.05 M NaCl, which means that an increase in the ionic strength resulted in narrower particle size distributions. Since a narrow size distribution is of great importance in the development of a drug delivery system, the particles prepared at high sodium chloride concentrations may be preferred. Moreover, it can be beneficial that the particles are prepared at physiological ionic strengths, which may reduce the loss of particle integrity after administration, as already mentioned in section 6.1. Thus, the chitosan particles prepared at the isotonic salt concentration of 0.15 M NaCl may be preferred in future studies on chitosan nanoparticles for possible drug delivery applications.

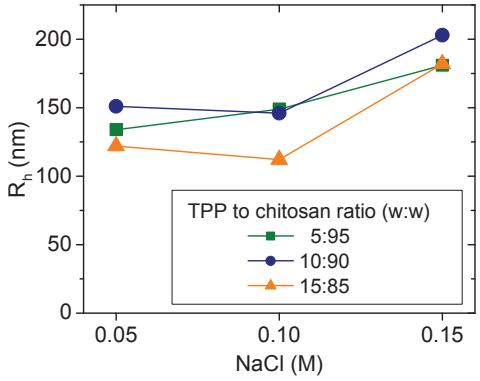


*Figure 6.5 – The average $R_h$ of chitosan nanoparticles prepared at three different TPP to chitosan ratios as a function of the NaCl concentration. Connection lines between the symbols are given in order to guide the eyes. The deviations of $R_h$ are approximately within the size of the symbols.*

The effects of the chitosan concentration on the average $R_h$ of chitosan nanoparticles prepared in the presence of sodium chloride are given in Figure 6.6. As can be seen from the figure, the particle size goes through a maximum with increasing crosslinker to chitosan ratios at a high chitosan concentration. In contrast, at a low chitosan concentration, no effects on the particle size were observed at low to moderate TPP to chitosan ratios, but a small drop in the particle size was observed at the highest ratio (Figure 6.6). In the crosslinking process, two opposing mechanisms are occurring simultaneously: 1) inter-crosslinking between different polymer chains and entities supporting a size increase, and 2) intra-crosslinking within the same polymer coil or particle leading to particle contraction and a size decrease. The variations in the particle size with increasing TPP to chitosan ratios may thus be explained by a sensitive relationship between these two mechanisms, which in some cases lead to a net cancellation and a constant particle size and in other cases a small decrease or increase in the particle size (Figure 6.6). It was also observed a tendency towards narrower particle size distributions (higher β values) with increasing TPP to chitosan ratios.

The average $R_h$ of the chitosan nanoparticles prepared were smaller (approximately 70 to 220 nm) than the self-associated and the crosslinked pectin nanoparticles (approximately 230 to 360 nm), see Figure 6.6 and Figure 6.3, respectively.

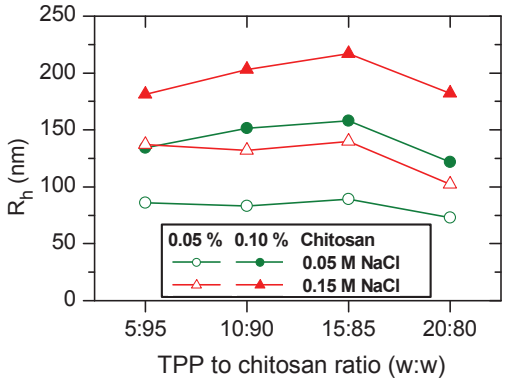


*Figure 6.6 – The average $R_h$ of chitosan nanoparticles prepared in the presence of NaCl as a function of TPP to chitosan ratio. Connection lines between the symbols are given in order to guide the eyes. The standard deviations of $R_h$ are equal to or smaller than the size of the symbols.*

Moreover, the particles based on LM-pectin were smaller than the ones based on AM-pectin. This may be due to the fact that the AM-pectin used had a higher $M_w$ than the LM-pectin, promoting enhanced polymer chain entanglements and a size increase. Gan et al. [61] found for instance in their work on ionically crosslinked chitosan nanoparticles that an increase in the molecular weight of the polysaccharide resulted in formation of larger particles. However, the chitosan nanoparticles prepared in this work were smaller than the pectin nanoparticles (compare Figure 6.6 and Figure 6.3), despite the considerably higher $M_w$ of chitosan. This can indicate two things, firstly that the pectin has a higher tendency of inter-chain association by other mechanisms than polymer chain entanglements (possibly hydrophobic associations of the methoxyl-esterified carboxyl groups), and secondly that the chitosan nanoparticles are more densely packed than the pectin nanoparticles. The results presented in section 6.2.3 on the effects on the particle compactness can verify the latter hypothesis.

Similar to the β value, the PDI value (ranging from 0 to 1) gives a measure of the particle size distribution. The major practical difference is that high PDI values correspond to wide size distributions in stead of narrow distributions. In the studies on pectin nanoparticles it was found that the self-associated LM-pectin nanoparticles had a bimodal size distribution, and an apparent PDI value close to 1. In contrast, the crosslinked LM-pectin nanoparticles had a unimodal size distribution and a PDI value of approximately 0.6. Both the self-associated and the crosslinked AM-pectin nanoparticles had unimodal size distributions and lower PDI values (≈ 0.3) when compared to the LM-pectin nanoparticles. If analyzing the DLS data in paper IV in the same manner as for the chitosan nanoparticles, the β value obtained was approximately 0.9. This means that a PDI value of 0.3 corresponds to a β value of approximately 0.9. Consequently, the AM-pectin nanoparticles and the chitosan nanoparticles prepared at the same sodium chloride concentration (0.05 M) exhibited similar size polydispersities, with the chitosan nanoparticles exhibiting β values in the range 0.85-0.94 and the AM-pectin nanoparticles an approximate β value of 0.9.

In paper II, it was found that larger particles were formed at a concentration of 0.10% chitosan if compared to 0.05%. This was observed at all ionic strengths and TPP to chitosan ratios studied. This concentration-induced size increase has been reported in several previous studies on chitosan-TPP nanoparticles [61-63, 67] and was expected given the greater likelihood of contact between polysaccharide chains at higher concentrations.

Of the two different types of pectin, AM-pectin was considered more promising due to the narrower particle size distributions observed. Further studies on the effects of the AM-pectin concentration on the particle characteristics were therefore performed. Figure 6.7 depicts the average $R_h$ of the self-associated and the crosslinked AM-pectin nanoparticles as a function of AM-pectin concentration. From the figure it can be observed an increase in the particle size of the self-associated AM-pectin nanoparticles with increasing pectin concentrations. This is in agreement with the above mentioned enhancement in inter-chain interactions and aggregation tendency at higher polymer concentrations. The particle size of the crosslinked AM-pectin nanoparticles, however, was slightly reduced when the pectin concentration increased from 0.03% to 0.05%, but found to be constant upon further increase to 0.07% pectin. Such peculiar effects on the particle size were also observed for the chitosan nanoparticles at increasing TPP to chitosan concentrations, and accordingly, the findings can be explained by a sensitive relationship between the two opposing crosslinking mechanisms occurring, i.e., intra-particle and inter-particle crosslinking. No significant differences in the PDI values of the AM-pectin nanoparticles were observed in the AM-pectin concentration range studied (PDI ≈ 0.3; corresponding to a β value of approximately 0.9).

To summarize the above: both the chitosan and the pectin nanoparticles prepared in the presence of sodium chloride were in the nanometer size range, and the results demonstrate the possibility of adjusting the particle size and size distribution by changing either the type of polysaccharide, the polysaccharide concentration, the ionic strength of the solvent and/or the crosslinker to polysaccharide ratio applied in the particle preparation.

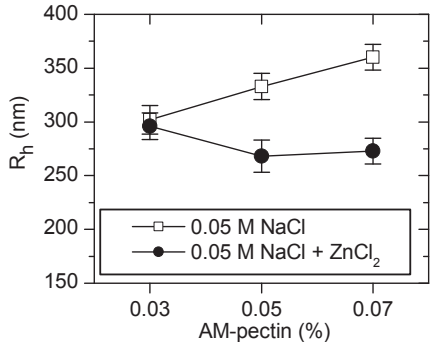


*Figure 6.7 – The average $R_h$ of self-associated and crosslinked AM-pectin nanoparticles as a function of AM-pectin concentration. Connection lines between the symbols are given in order to guide the eyes. The $ZnCl_2$ to pectin weight ratio was 15:85.*

### 6.2.2 Charge

As can be seen from Figure 6.8, all the chitosan nanoparticles were positively charged, which is in accordance with several previous studies on chitosan-TPP nanoparticles [58, 60, 107, 108]. In contrast to the positively charged chitosan nanoparticles, the self-associated and the crosslinked pectin nanoparticles were negatively charged (see Figure 6.9). The pH of the dispersions were around or below the $pK_a$ value of the amine groups of chitosan (~6.5), and around or above the $pK_a$ value of the carboxyl groups of pectin (~ 3.5), thus stimulating ionization and the observed positive and negative zeta potentials, respectively.

The TPP anions will, as a result of the crosslinking process, neutralize some of chitosan's positive charges. An increase in the TPP to chitosan ratio was thus expected to reduce the average zeta potential values of the chitosan particles, and this was clearly observed for the particles prepared in pure water (see Figure 6.8). In the presence of sodium chloride, however, this effect was rather moderate in comparison. Moreover, at low to moderate TPP to chitosan ratios, a significant decrease in the zeta potential values was observed if prepared in the presence of sodium chloride (with respect to pure water). These results are in accordance with the proposed salt-induced screening of the electrostatic charges and are also in agreement with the findings of Huang and Lapitsky [58] in their recent study on chitosan-TPP nanoparticles.

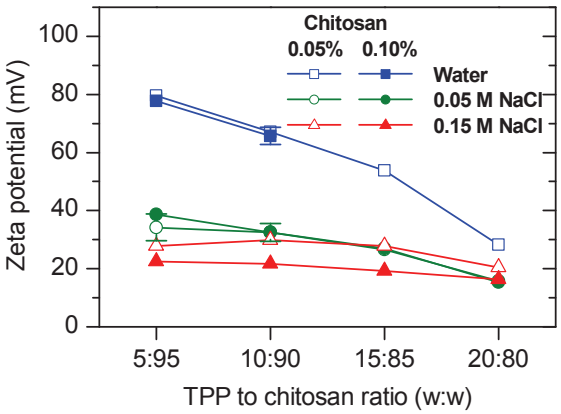


*Figure 6.8 – The average zeta potential of chitosan nanoparticles as a function of TPP to chitosan ratio. Connection lines are given in order to guide the eyes. Samples in which particle sedimentation was observed are omitted from the figure. The points without error bars have standard deviations equal to or smaller than the size of the symbols.*

The crosslinked pectin nanoparticles exhibited lower absolute zeta potential values than the self-associated nanoparticles (Figure 6.9). This is in accordance with the proposed crosslinking mechanism where the positively charged divalent $Zn^{2+}$-ions electrostatically interact with negatively charged carboxyl groups, thus reducing the amount of charged species and the absolute value of the particles' zeta potential.

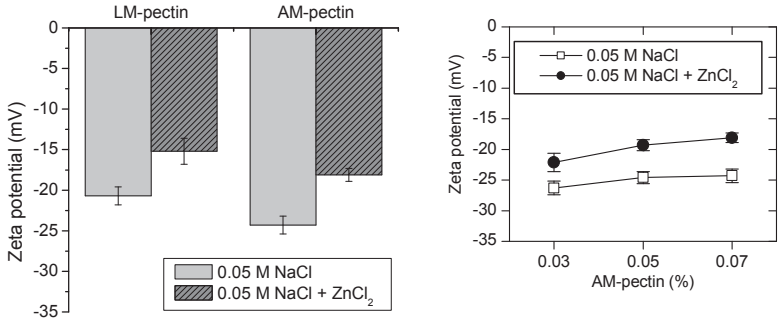


*Figure 6.9 – Left: The average zeta potential values of self-associated and crosslinked LM-pectin and AM-pectin nanoparticles prepared at 0.07% pectin. Right: The average zeta potential values of self-associated and crosslinked AM-pectin nanoparticles as a function of AM-pectin concentration (connection lines between the symbols are given in order to guide the eyes). The $ZnCl_2$ to pectin weight ratio was 15:85.*

### 6.2.3 Compactness

The work performed in paper I describes a theoretical method for the calculation of the local polymer concentration inside nanoparticles ($c_{NP}$) by combining data from size and turbidity measurements. This work enabled the calculation of the $c_{NP}$ as a measure of the particle compactness in the following papers II-IV. Increasing $c_{NP}$ values correspond to higher particle compactness.

Figure 6.10 depicts the local polymer concentrations inside the chitosan nanoparticles ($c_{NP}$) studied in paper II as a function of the TPP to chitosan ratio. At moderate to high TPP to chitosan ratios, a distinct increase in the $c_{NP}$ was observed with an increase in the sodium chloride concentration. This relates well with the proposed charge screening effect of monovalent salts and the resultant polymer conformation change illustrated in Figure 6.1 (page 31). As expected, a marked increase in the $c_{NP}$ was also found with increasing TPP to chitosan ratios, whereas the $c_{NP}$ was found to be unaffected by the chitosan concentration at low to moderate TPP to chitosan ratios. Interestingly, at the highest TPP to chitosan ratio of 20:80, the $c_{NP}$ increased when adjusting the chitosan concentration from 0.05% to 0.10%.

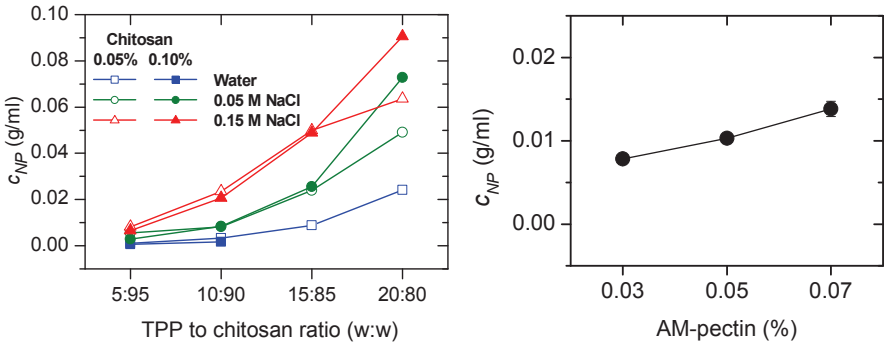


*Figure 6.10 – Left: The local polymer concentration inside chitosan nanoparticles as a function of TPP to chitosan ratio. Samples in which particle sedimentation was observed are omitted from the figure. Right: The local polymer concentration inside crosslinked AM-pectin nanoparticles as a function of AM-pectin concentration. The $ZnCl_2$ to pectin weight ratio was 15:85. Connection lines between the symbols are given in order to guide the eyes.*

This observation can be explained by an ionic strength effect: changing the chitosan concentration while keeping the TPP to chitosan ratio constant will naturally lead to an increase in the TPP concentration, and thus the ionic strength of the solution. At some point, this contribution to the ionic strength may enhance the contraction tendency of the chitosan, resulting in higher $c_{NP}$ values.

For the pectin nanoparticles studied in paper IV, the $c_{NP}$ was estimated for the crosslinked AM-pectin nanoparticles prepared at 0.05 M NaCl and a $ZnCl_2$ to pectin ratio of 15:85. The $c_{NP}$ values of these particles as a function of the AM-pectin concentration are given in Figure 6.10. Interestingly, as can be seen in the figure, increasing AM-pectin concentrations lead to increasing $c_{NP}$ values. As mentioned above, this may be an effect induced by the proportional increase in the $ZnCl_2$ concentration with increasing pectin concentrations, leading to higher ionic strengths and an enhanced salting-out effect or contraction of the polymer entities in solution.

The chitosan nanoparticles were generally found to be more compact (higher $c_{NP}$ values) than the AM-pectin nanoparticles, and can partly explain why the chitosan nanoparticles were found to be smaller than the pectin nanoparticles, as already presented in section 6.2.1.

## 6.3 Stability in suspension

The results presented in sections 6.1 and 6.2 clearly illustrate the potential and benefits of preparing chitosan and pectin based nanoparticles in the presence of sodium chloride. The absolute zeta potential values of both the chitosan and the pectin nanoparticles prepared under saline conditions were, however, predominately below 30 mV. As a rule of thumb, zeta potential values above an absolute value of 30 mV are considered necessary for good colloidal stability [99-101]. The stability of the particles towards changes in the size and compactness were therefore studied in paper III (chitosan) and IV (pectin) over a period of one month.

The average $R_h$ and the $c_{NP}$ values of the chitosan nanoparticles prepared in the presence of sodium chloride as a function of time are given in Figure 6.11 and Figure 6.12, respectively. Generally, only minor changes in the $R_h$ or the $c_{NP}$ (less than 10%) were observed.

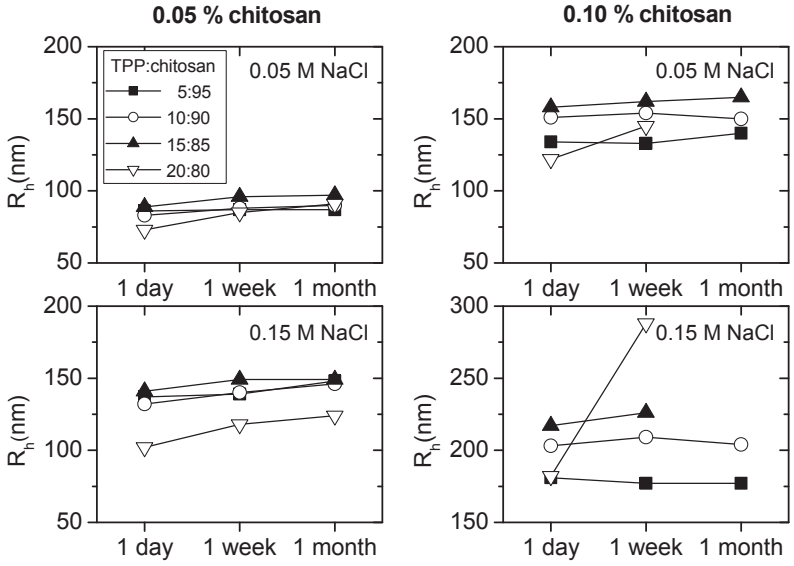


*Figure 6.11 – The average $R_h$ of chitosan nanoparticles prepared in the presence of sodium chloride at 0.05% chitosan (left) and 0.10% chitosan (right) as a function of time. Connection lines between the symbols are given in order to guide the eyes. Samples in which particle sedimentation was observed are omitted from the figure.*

The chitosan nanoparticles that were found to be unstable over time, reflected as a change in the $R_h$ or $c_{NP}$, or by particle sedimentation, were prepared at 1) a high TPP to chitosan ratio, 2) a high chitosan concentration and/or 3) a high sodium chloride concentration. Accordingly, the decreased zeta potentials found at high TPP to chitosan ratios (see Figure 6.8), increased the possibility of particle aggregation over time. Moreover, the initial higher $c_{NP}$ values (Figure 6.10) and larger sizes (Figure 6.6) of the unstable combinations promoted particle sedimentation and instability. The self-associated AM-pectin nanoparticles prepared at a pectin concentration of 0.07% in the presence of 0.05 M NaCl were also found to be stable over a one month period. However, the AM-pectin nanoparticles crosslinked with $ZnCl_2$ were only found to be stable after one week of storage: after one month aggregated flakes/flocs were observed in the samples. This increased aggregation tendency is most likely linked to the lower absolute zeta potential values found for these particles, if compared to both the self-associated AM-pectin nanoparticles and the chitosan nanoparticles (Figure 6.9 and Figure 6.8, respectively).

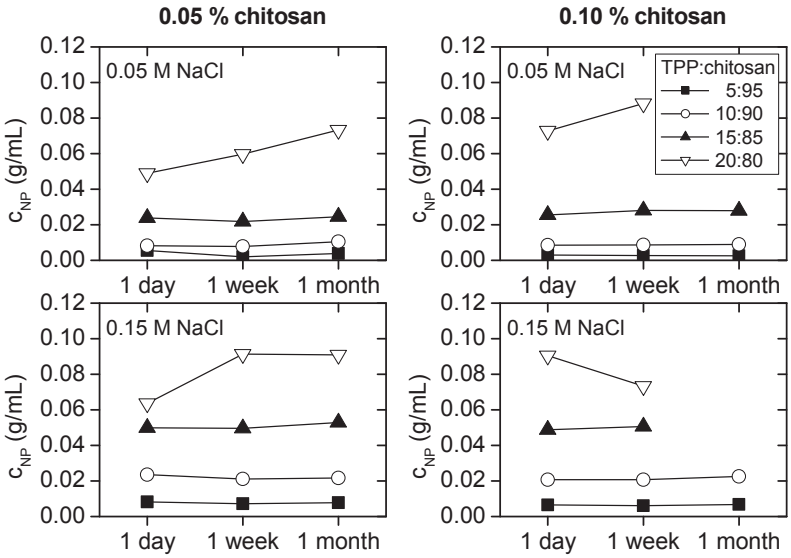


*Figure 6.12 – The local polymer concentration inside chitosan nanoparticles prepared in the presence of sodium chloride at 0.05% chitosan (left) and 0.10% chitosan (right) as a function of time. Connection lines between the symbols are given in order to guide the eyes. Samples in which particle sedimentation was observed are omitted from the figure.*

As can be seen in Figure 6.11 and Figure 6.12, the unstable chitosan particles increased in size and compactness over time, except for one of the combinations that was found to be larger, but less compact after one week of storage. This combination was prepared at the most "extreme" conditions, and also exhibited the highest initial $c_{NP}$ value. Since aggregation and coalescence of nanoparticles is suppressed at sufficiently high $c_{NP}$ [109, 110], it was proposed that the aggregates formed for this combination consisted of "hard spheres" packed together with open voids in-between the particles (paper III), which would explain the observed increase in size and decrease in particle compactness. This kind of aggregate structure was recently observed for chitosan-TPP-nanoparticles in a study of Huang and Lapitsky[111], and has also been proposed for other polymer systems [112].

## 6.4 Interaction with mucin

In order to evaluate the nanoparticles' potential mucoadhesive properties, the in vitro interaction of mucin with two selected combinations of nanoparticles was studied. The nanoparticles were prepared in 0.05 M NaCl, at a polysaccharide concentration of 0.05% and a crosslinker to polysaccharide ratio of 15:85. In Figure 6.13, it can be observed that the vial containing chitosan nanoparticles mixed with mucin (vial marked with C+M), was quite turbid if compared to the vials containing chitosan nanoparticles (vial C) and mucin solution (vial M). Large flocs/aggregates could be seen by the naked eye, and these structures started to settle if left standing. In contrast, the mixture of AM-pectin nanoparticles with mucin (vial P+M) was not significantly more turbid than the controls (vial M and P) if controlled by the naked eye.

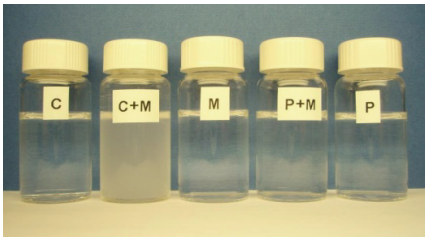


*Figure 6.13 – Vials containing (C) chitosan nanoparticles, (C+M) chitosan nanoparticles mixed with mucin, (M) mucin solution, (P+M) AM-pectin nanoparticles mixed with mucin, and (P) AM-pectin nanoparticles. The samples were homogeneous without any sign of phase separation (except for sample C+M, in which particle sedimentation was observed after some minutes if left standing); the apparent turbidity increase at the bottom of the samples is merely a photographic artefact.*

In Table 6.1, the average $R_h$, PDI, zeta potential and transmittance values of the AM-pectin samples are displayed, along with the pH of the sample. No significant difference in the $R_h$ of the AM-pectin nanoparticles and the mixture of AM-pectin nanoparticles and mucin can be observed. Furthermore, only a slight decrease in the transmittance was found. Consequently, the AM-pectin nanoparticles' potential to interact with mucin appears rather low from these experiments. However, Klemetsrud et al. [98] have previously shown, by applying a similar method, that liposomes coated with AM-pectin interact with mucin. In these studies, the concentration of mucin solution was higher and the pectin was not crosslinked at the liposome surface, thus increasing the possibility for polymer chain entanglement. This may explain the different results obtained, since polymer entanglement has been indicated as an important interaction mechanism between pectin and mucin [113-115]. Accordingly, pectin gel beads with increasing degrees of crosslinking, and thus less flexible and mobile chains, have been shown to be less mucoadhesive [91]. Chitosan, on the other hand, interacts strongly with mucin by electrostatic interactions [116], explaining the observed differences between the two types of polysaccharide based nanoparticles.

*Table 6.1 – Overview of the sample characteristics obtained in the in vitro interaction studies between crosslinked AM-pectin nanoparticles and mucin (n=3).*

| Vial | $R_h$ (nm) | PDI | Transmittance (%) | Zeta potential (mV) | pH |
|---|---|---|---|---|---|
| Mucin **(M)** | 258 ± 10 | 0.62 ± 0.02 | 99.2 | -19.5 ± 1.3 | 6.6 |
| AM-pectin NPs **(P)** | 306 ± 14 | 0.32 ± 0.04 | 98.0 | -21.1 ± 1.2 | 4.0 |
| AM-pectin NPs + mucin **(P+M)** | 301 ± 11 | 0.35 ± 0.05 | 96.5 | -19.6 ± 0.8 | 4.1 |

# 7 Concluding remarks

The size, charge and compactness are important physicochemical properties of nanoparticulate drug delivery systems, linked to both mucus interaction and penetration [24, 25], systemic distribution [10, 29] and drug release rates [33-35]. The particle compactness is, however, seldom reported in studies on polysaccharide and polymer based nanoparticles, probably due to experimental difficulties in estimating this parameter [117]. The particles prepared in this work were characterized with respect to particle size and charge by well-known methods, while a theoretical method was developed in order to estimate the particle compactness (paper I). This method combines data from DLS and turbidity measurements to calculate the local polymer concentration inside the nanoparticles ($c_{NP}$), as a measure of the particle compactness. The method is developed for spherical, monodisperse particles, and the total polymer concentration that exists in the form of nanoparticles must be known. These considerations could be assumed for both the crosslinked chitosan and pectin nanoparticles prepared in the presence of sodium chloride. This theoretically deduced method has also been adapted indirectly [98, 118] or directly [119] in other papers to discuss the compactness of polysaccharide or polymer based nanoparticulate systems.

The results obtained in this thesis demonstrate that nanoparticles based on the polysaccharides chitosan and pectin could be prepared by ionotropic gelation with multivalent ions in the presence of sodium chloride. In pure water, however, chitosan microparticles or a macroscopic pectin network was formed instead of the desired nanoparticles. It was also found that non-crosslinked, self-associated pectin nanoparticles could be prepared in the absence of divalent cations (i.e., in the presence of sodium chloride only). All these observations can be explained by a change in the polysaccharide chain conformation and association in the presence of monovalent salt. Consequently, it can be concluded the solvent salinity is an important parameter to address in the preparation of nanoparticulate DDSs based on chitosan and pectin.

It was also found that the nanoparticles' physicochemical properties could be easily adjusted by varying the solvent salinity, the type and concentration of polysaccharide, and the crosslinker to polysaccharide ratio. Specifically, by changing the sodium chloride concentration of the solvent used in the particle preparation from 0.05 to 0.15 M, the average particle size and compactness of the chitosan nanoparticles were raised. Increasing the TPP to chitosan ratio, however, only moderately affected the average particle size, but

lead to a significant increase in the particle compactness. The chitosan concentration did not affect the particle compactness at low to moderate TPP to chitosan ratios, but significantly affected the particle size. This latter observation points out the possibility of preparing chitosan nanoparticles of different particle sizes, but of equal particle compactness by simply adjusting the chitosan concentration. Interestingly, increasing the AM-pectin concentrations resulted in a size increase of the self-associated nanoparticles, but not of the crosslinked nanoparticles. This lack in size increase of the crosslinked AM-pectin nanoparticles was concurrent with an increase in the particle compactness and explained by a sensitive relationship between intra- and inter-particle crosslinking. The main difference between the chitosan and the pectin nanoparticles prepared was that they exhibited positive and negative zeta potentials, respectively. Moreover, the chitosan nanoparticles were generally smaller and more compact than the pectin nanoparticles.

Despite the reduced absolute zeta potential values of the nanoparticles prepared in the presence of sodium chloride, the chitosan and the pectin nanoparticles were mainly found to be colloidally stable after one week of storage. Several of the nanoparticle suspensions could also be stored for an entire month without significant changes in the average particle size, charge and compactness. The fact that the nanoparticles are stable in suspension for several days may facilitate simple screening studies because the extra preparation step of freeze-drying can be avoided.

The positively charged chitosan nanoparticles interacted strongly with the negatively charged mucin in vitro. This indicates that the chitosan nanoparticles are likely to be immobilized in the more rapidly cleared upper part of the mucus layer [25], despite being relatively small. In contrast, the negatively charged pectin nanoparticles showed little interaction with mucin in vitro, and may thus possibly penetrate deeper in the mucus mesh, given that the pore size at the mucosal site is sufficiently large.

The results obtained in this thesis can be used as a guide in future studies on nanoparticles based on chitosan and pectin, and possibly other polysaccharides with polyelectrolyte properties, such as alginate and hyaluronic acid.

# 8 Future perspectives

The underlying basis of this work was that nanoparticles based on mucoadhesive polysaccharides can possibly improve drug treatment locally or enhance the systemic delivery of drugs after administration to mucosal routes. There are several mucosal administration routes with a need for improvement in local therapy, or where the administration of drugs for systemic effects would be appropriate [7, 8, 24, 25, 40, 120-124]. The nasal route is one good example studied for local delivery of vaccines, and for direct nose-to-brain delivery through the olfactory region [123].

The findings in this thesis offer a decent platform for further studies on the applicability of polysaccharide based nanoparticles for drug delivery purposes. However, several future studies should be performed to obtain an improved understanding of polysaccharide based nanoparticles as a DDS. One of the major findings in this study was that the ionic strength had a tremendous effect on the particle preparation and particle characteristics, which could mainly be explained by a change in polysaccharide chain conformation. The influence of this conformational change on the encapsulation efficiency of drugs into the particles was out of the scope of this thesis; however, it is tempting to assume that the drug encapsulation process will be affected as well. It would thus be interesting to look into the possible impacts of the ionic strength and the particle compactness on the encapsulation and release rates of drugs with various charge and molecular weights.

Moreover, studies investigating the fate of the nanoparticles in the human body post mucosal administration can highly contribute to the evaluation of their suitability as DDSs for local or systemic delivery. As a first step, the mucoadhesive properties of the nanoparticles could be evaluated further in vitro or ex vivo in the presence of a suitable isotonic buffer or simulated body fluid. This would be especially interesting for the AM-pectin nanoparticles that showed few signs of interaction with mucin under the present experimental conditions. Evaluation of the particles' toxicity profile in vitro using suitable mucosal cell lines should also be performed, before the fate and action of the DDSs were to be evaluated for a specific application in vivo.

# 9 References


1. Lalla RV, Bensadoun R-J. *Miconazole mucoadhesive tablet for oropharyngeal candidiasis*, Expert Rev Anti Infect Ther 2010; 9(1): 13-17.

2. Vazquez JA, Patton LL, Epstein JB, Ramlachan P, Mitha I, Noveljic Z, Fourie J, Conway B, Lalla RV, Barasch A, Attali P. *Randomized, comparative, double-blind, double-dummy, multicenter trial of miconazole buccal tablet and clotrimazole troches for the treatment of oropharyngeal candidiasis: study of miconazole Lauriad® efficacy and safety (SMiLES)*, HIV Clin Trials 2010; 11(4): 186-96.

3. Guevara-Aguirre J, Guevara M, Saavedra J, Mihic M, Modi P. *Beneficial effects of addition of oral spray insulin (Oralin) on insulin secretion and metabolic control in subjects with type 2 diabetes mellitus suboptimally controlled on oral hypoglycemic agents*, Diabetes Technol Ther 2004; 6(1): 1-8.

4. Guevara-Aguirre J, Guevara-Aguirre M, Saavedra J, Bernstein G, Rosenbloom AL. *Comparison of oral insulin spray and subcutaneous regular insulin at mealtime in type 1 diabetes*, Diabetes Technol Ther 2007; 9(4): 372-6.

5. Hillery AM, Lloyd AW, Swarbrick J, eds. *Drug delivery and targeting for pharmacists and pharmaceutical scientists*. 2001, Taylor & Francis: London.

6. Tiwari G, Tiwari R, Sriwastawa B, Bhati L, Pandey S, Pandey P, Bannerjee SK. *Drug delivery systems: An updated review*, Int J Pharm Investig 2012; 2(1): 2-11.

7. Bhattarai N, Gunn J, Zhang M. *Chitosan-based hydrogels for controlled, localized drug delivery*, Adv Drug Del Rev 2010; 62(1): 83-99.

8. Csaba N, Garcia-Fuentes M, Alonso MJ. *Nanoparticles for nasal vaccination*, Adv Drug Del Rev 2009; 61(2): 140-157.

9. Koo H, Huh MS, Sun I-C, Yuk SH, Choi K, Kim K, Kwon IC. *In vivo targeted delivery of nanoparticles for theranosis*, Acc Chem Res 2011; 44(10): 1018-1028.

10. Raemdonck K, Martens TF, Braeckmans K, Demeester J, De Smedt SC. *Polysaccharide-based nucleic acid nanoformulations*, Adv Drug Del Rev 2013; 65(9): 1123-1147.

11. Liu Z, Jiao Y, Wang Y, Zhou C, Zhang Z. *Polysaccharides-based nanoparticles as drug delivery systems*, Adv Drug Del Rev 2008; 60(15): 1650-1662.

12. Bamrungsap S, Zhao Z, Chen T, Wang L, Li C, Fu T, Tan W. *Nanotechnology in therapeutics: a focus on nanoparticles as a drug delivery system*, Nanomedicine 2012; 7(8): 1253-1271.

13. Kohane DS. *Microparticles and nanoparticles for drug delivery*, Biotechnol Bioeng 2007; 96(2): 203-209.

14. Merisko-Liversidge EM, Liversidge GG. *Drug nanoparticles: formulating poorly water-soluble compounds*, Toxicol Pathol 2008; 36(1): 43-48.

15. Fröhlich E, Roblegg E. *Models for oral uptake of nanoparticles in consumer products*, Toxicology 2012; 291(1–3): 10-17.

16. Plapied L, Duhem N, des Rieux A, Préat V. *Fate of polymeric nanocarriers for oral drug delivery*, Curr Opin Colloid Interface Sci 2011; 16(3): 228-237.

17. Ravi Kumar MNV, Muzzarelli RAA, Muzzarelli C, Sashiwa H, Domb AJ. *Chitosan chemistry and pharmaceutical perspectives*, Chem Rev 2004; 104(12): 6017-6084.

18. Yang S-G. *Biowaiver extension potential and IVIVC for BCS Class II drugs by formulation design: Case study for cyclosporine self-microemulsifying formulation*, Arch Pharm Res 2010; 33(11): 1835-1842.

19. Müller RH, Runge S, Ravelli V, Mehnert W, Thünemann AF, Souto EB. *Oral bioavailability of cyclosporine: Solid lipid nanoparticles (SLN®) versus drug nanocrystals*, Int J Pharm 2006; 317(1): 82-89.

20. Balmayor E, Azevedo H, Reis R. *Controlled delivery systems: from pharmaceuticals to cells and genes*, Pharm Res 2011; 28(6): 1241-1258.

21. Liechty WB, Kryscio DR, Slaughter BV, Peppas NA. *Polymers for drug delivery systems*, Annu Rev Chem Biomol Eng 2010; 1(1): 149-173.

22. Cui F-d, Tao A-j, Cun D-m, Zhang L-q, Shi K. *Preparation of insulin loaded PLGA-Hp55 nanoparticles for oral delivery*, J Pharm Sci 2007; 96(2): 421-427.

23. Aggarwal P, Hall JB, McLeland CB, Dobrovolskaia MA, McNeil SE. *Nanoparticle interaction with plasma proteins as it relates to particle biodistribution, biocompatibility and therapeutic efficacy*, Adv Drug Del Rev 2009; 61(6): 428-437.

24. Ensign LM, Cone R, Hanes J. *Oral drug delivery with polymeric nanoparticles: The gastrointestinal mucus barriers*, Adv Drug Del Rev 2012; 64(6): 557-570.

25. Lai SK, Wang Y-Y, Hanes J. *Mucus-penetrating nanoparticles for drug and gene delivery to mucosal tissues*, Adv Drug Del Rev 2009; 61(2): 158-171.

26. Norris DA, Sinko PJ. *Effect of size, surface charge, and hydrophobicity on the translocation of polystyrene microspheres through gastrointestinal mucin*, J Appl Polym Sci 1997; 63(11): 1481-1492.

27. Suk JS, Lai SK, Wang Y-Y, Ensign LM, Zeitlin PL, Boyle MP, Hanes J. *The penetration of fresh undiluted sputum expectorated by cystic fibrosis patients by non-adhesive polymer nanoparticles*, Biomaterials 2009; 30(13): 2591-2597.

28. Lai SK, O'Hanlon DE, Harrold S, Man ST, Wang Y-Y, Cone R, Hanes J. *Rapid transport of large polymeric nanoparticles in fresh undiluted human mucus*, Proc Natl Acad Sci USA 2007; 104(5): 1482-1487.

29. Petros RA, DeSimone JM. *Strategies in the design of nanoparticles for therapeutic applications*, Nat Rev Drug Discov 2010; 9(8): 615-627.

30. Li S-D, Huang L. *Stealth nanoparticles: High density but sheddable PEG is a key for tumor targeting*, J Control Release 2010; 145(3): 178-181.

31. Ding H-M, Ma Y-Q. *Controlling cellular uptake of nanoparticles with pH-sensitive polymers*, Sci Rep 2013; 3: 2804.

32. Alvarez-Lorenzo C, Blanco-Fernandez B, Puga AM, Concheiro A. *Crosslinked ionic polysaccharides for stimuli-sensitive drug delivery*, Adv Drug Del Rev 2013; 65(9): 1148-1171.

33. Chouhan R, Bajpai AK. *Release dynamics of ciprofloxacin from swellable nanocarriers of poly(2-hydroxyethyl methacrylate): an in vitro study*, Nanomedicine 2010; 6: 453-462.

34. Kim S, Kim J-H, Kim D. *pH sensitive swelling and releasing behavior of nano-gels based on polyaspartamide graft copolymers*, J Colloid Interface Sci 2011; 356: 100-106.

35. Polakovič M, Görner T, Gref R, Dellacherie E. *Lidocaine loaded biodegradable nanospheres: II. Modelling of drug release*, J Control Release 1999; 60(2–3): 169-177.

36. De Jong WH, Borm PJ. *Drug delivery and nanoparticles: Applications and hazards*, Int J Nanomedicine 2008; 3(2): 133-49.

37. Attwood D, *Disperse systems*, in *Pharmaceutics: The science of dosage form design*, Aulton ME, ed. 2002, Churchill Livingstone: Edinburgh. 70-100.

38. Florence AT, Attwood D, *Physicochemical principles of pharmacy*. 3rd ed. 1998, Pharmaceutical Press: London.

39. Zhang G, Wu C. *Folding and formation of mesoglobules in dilute copolymer solutions*, Adv Polym Sci 2006; 195: 101-176.

40. Yun Y, Cho YW, Park K. *Nanoparticles for oral delivery: Targeted nanoparticles with peptidic ligands for oral protein delivery*, Adv Drug Del Rev 2013; 65(6): 822-832.

41. Dünnhaupt S, Barthelmes J, Hombach J, Sakloetsakun D, Arkhipova V, Bernkop-Schnürch A. *Distribution of thiolated mucoadhesive nanoparticles on intestinal mucosa*, Int J Pharm 2011; 408(1–2): 191-199.

42. Langer R. *Drug delivery and targeting*, Nature 1998; 392(6679 Suppl): 5-10.

43. Augst AD, Kong HJ, Mooney DJ. *Alginate hydrogels as biomaterials*, Macromolecular Bioscience 2006; 6(8): 623-633.

44. Kean T, Thanou M. *Biodegradation, biodistribution and toxicity of chitosan*, Adv Drug Del Rev 2010; 62(1): 3-11.

45. Yang L, Chu JS, Fix JA. *Colon-specific drug delivery: new approaches and in vitro/in vivo evaluation*, Int J Pharm 2002; 235(1-2): 1-15.

46. Sande SA. *Pectin-based oral drug delivery to the colon*, Expert Opin Drug Deliv 2005; 2(3): 441-450.

47. Sriamornsak P. *Application of pectin in oral drug delivery*, Expert Opin Drug Deliv 2011; 8(8): 1009-1023.

48. Liu L, Fishman ML, Kost J, Hicks KB. *Pectin-based systems for colon-specific drug delivery via oral route*, Biomaterials 2003; 24(19): 3333-3343.

49. Sinha VR, Kumria R. *Polysaccharides in colon-specific drug delivery*, Int J Pharm 2001; 224(1-2): 19-38.

50. Zhang H, Ma Y, Sun X-L. *Recent developments in carbohydrate-decorated targeted drug/gene delivery*, Med Res Rev 2010; 30(2): 270-289.

51. George M, Abraham TE. *Polyionic hydrocolloids for the intestinal delivery of protein drugs: Alginate and chitosan -- a review*, J Control Release 2006; 114(1): 1-14.

52. Vauthier C, Bouchemal K. *Methods for the preparation and manufacture of polymeric nanoparticles*, Pharm Res 2009; 26(5): 1025-1058.

53. Dash M, Chiellini F, Ottenbrite RM, Chiellini E. *Chitosan--A versatile semi-synthetic polymer in biomedical applications*, Prog Polym Sci 2011; 36(8): 981-1014.

54. Bodnar M, Hartmann JF, Borbely J. *Preparation and characterization of chitosan-based nanoparticles*, Biomacromolecules 2005; 6(5): 2521-2527.

55. Hamidi M, Azadi A, Rafiei P. *Hydrogel nanoparticles in drug delivery*, Adv Drug Del Rev 2008; 60(15): 1638-1649.

56. Calvo P, Remuñán-López C, Vila-Jato JL, Alonso MJ. *Novel hydrophilic chitosan-polyethylene oxide nanoparticles as protein carriers*, J Appl Polym Sci 1997; 63(1): 125-132.

57. Lin Y-H, Sonaje K, Lin KM, Juang J-H, Mi F-L, Yang H-W, Sung H-W. *Multi-ion-crosslinked nanoparticles with pH-responsive characteristics for oral delivery of protein drugs*, J Control Release 2008; 132(2): 141-149.

58. Huang Y, Lapitsky Y. *Monovalent salt enhances colloidal stability during the formation of chitosan/tripolyphosphate microgels*, Langmuir 2011; 27(17): 10392-10399.

59. Yang H-C, Hon M-H. *The effect of the molecular weight of chitosan nanoparticles and its application on drug delivery*, Microchem J 2009; 92(1): 87-91.

60. Janes KA, Alonso MJ. *Depolymerized chitosan nanoparticles for protein delivery: Preparation and characterization*, J Appl Polym Sci 2003; 88(12): 2769-2776.

61. Gan Q, Wang T, Cochrane C, McCarron P. *Modulation of surface charge, particle size and morphological properties of chitosan-TPP nanoparticles intended for gene delivery*, Colloids Surf B Biointerfaces 2005; 44(2-3): 65-73.

62. Liu H, Gao C. *Preparation and properties of ionically cross-linked chitosan nanoparticles*, Polym Adv Technol 2009; 20(7): 613-619.

63. Shah S, Pal A, Kaushik VK, Devi S. *Preparation and characterization of venlafaxine hydrochloride-loaded chitosan nanoparticles and in vitro release of drug*, J Appl Polym Sci 2009; 112(5): 2876-2887.

64. Opanasopit P, Apirakaramwong A, Ngawhirunpat T, Rojanarata T, Ruktanonchai U. *Development and characterization of pectinate micro/nanoparticles for gene delivery*, AAPS PharmSciTech 2008; 9(1): 67-74.

65. Ma Z, Yeoh HH, Lim L-Y. *Formulation pH modulates the interaction of insulin with chitosan nanoparticles*, J Pharm Sci 2002; 91: 1396-1404.

66. Zhang H, Oh M, Allen C, Kumacheva E. *Monodisperse chitosan nanoparticles for mucosal drug delivery*, Biomacromolecules 2004; 5(6): 2461-2468.

67. Tsai ML, Bai SW, Chen RH. *Cavitation effects versus stretch effects resulted in different size and polydispersity of ionotropic gelation chitosan-sodium tripolyphosphate nanoparticle*, Carbohydr Polym 2008; 71(3): 448-457.

68. Dong Y, Ng WK, Shen S, Kim S, Tan RB. *Scalable ionic gelation synthesis of chitosan nanoparticles for drug delivery in static mixers*, Carbohydr Polym 2013; 94(2): 940-5.

69. Berger J, Reist M, Mayer JM, Felt O, Peppas NA, Gurny R. *Structure and interactions in covalently and ionically crosslinked chitosan hydrogels for biomedical applications*, Eur J Pharm Biopharm 2004; 57(1): 19-34.

70. Buschmann MD, Merzouki A, Lavertu M, Thibault M, Jean M, Darras V. *Chitosans for delivery of nucleic acids*, Adv Drug Del Rev 2013; 65(9): 1234-1270.

71. Liu C-G, Desai KGH, Chen X-G, Park H-J. *Linolenic acid-modified chitosan for formation of self-assembled nanoparticles*, J Agric Food Chem 2004; 53(2): 437-441.

72. Rapoport N. *Physical stimuli-responsive polymeric micelles for anti-cancer drug delivery*, Prog Polym Sci 2007; 32(8–9): 962-990.

73. Hamman JH. *Chitosan based polyelectrolyte complexes as potential carrier materials in drug delivery systems*, Mar Drugs 2010; 8(4): 1305-1322.

74. Anthonsen MW, Smidsrød O. *Hydrogen ion titration of chitosans with varying degrees of N-acetylation by monitoring induced $^{1}$H-NMR chemical shifts*, Carbohydr Polym 1995; 26(4): 303-305.

75. Park JH, Saravanakumar G, Kim K, Kwon IC. *Targeted delivery of low molecular drugs using chitosan and its derivatives*, Adv Drug Del Rev 2010; 62(1): 28-41.

76. Leithner K, Bernkop-Schnürch A, *Chitosan and derivatives for biopharmaceutical use: Mucoadhesive properties*, in *Chitosan-based systems for biopharmaceuticals: delivery, targeting and polymer therapeutics*, Sarmento B, das Neves J, eds. 2012, John Wiley & Sons, Ltd: Chichester. 159-180.

77. Chuang C-Y, Don T-M, Chiu W-Y. *Synthesis of chitosan-based thermo- and pH-responsive porous nanoparticles by temperature-dependent self-assembly method and their application in drug release*, J Polym Sci A Polym Chem 2009; 47(19): 5126-5136.

78. Halim AS, Keong LC, Zainol I, Rashid AHAR, *Biocompatibility and biodegradation of chitosan and derivatives*, in *Chitosan-based systems for biopharmaceuticals: delivery, targeting and polymer therapeutics*, Sarmento B, das Neves J, eds. 2012, John Wiley & Sons, Ltd: Chichester. 55-73.

79. Kean TJ, Thanou M, *Toxicological properties of chitosan and derivatives for biopharmaceutical applications*, in *Chitosan-based systems for biopharmaceuticals: delivery, targeting and polymer therapeutics*, Sarmento B, das Neves J, eds. 2012, John Wiley & Sons, Ltd: Chichester. 453-461.

80. Mellegård H, Strand SP, Christensen BE, Granum PE, Hardy SP. *Antibacterial activity of chemically defined chitosans: Influence of molecular weight, degree of acetylation and test organism*, Int J Food Microbiol 2011; 148(1): 48-54.

81. Maeda Y, Kimura Y. *Antitumor effects of various low-molecular-weight chitosans are due to increased natural killer activity of intestinal intraepithelial lymphocytes in sarcoma 180–bearing mice*, J Nutr 2004; 134(4): 945-950.

82. Sarmento B, das Neves J, eds. *Chitosan-based systems for biopharmaceuticals: delivery, targeting and polymer therapeutics*. 2012, John Wiley & Sons, Ltd: Chichester.

83. Wang X, Zheng C, Wu Z, Teng D, Zhang X, Wang Z, Li C. *Chitosan-NAC nanoparticles as a vehicle for nasal absorption enhancement of insulin*, J Biomed Mater Res B Appl Biomater 2009; 88B(1): 150-161.

84. Wang X, Chi N, Tang X. *Preparation of estradiol chitosan nanoparticles for improving nasal absorption and brain targeting*, Eur J Pharm Biopharm 2008; 70(3): 735-740.

85. Elzatahry AA, Mohy Eldin MS. *Preparation and characterization of metronidazole-loaded chitosan nanoparticles for drug delivery application*, Polym Adv Technol 2008; 19(12): 1787-1791.

86. BeMiller James N, *An Introduction to Pectins: Structure and Properties*, in *Chemistry and Function of Pectins*, Fishman ML, Jen JJ, eds. 1986, American Chemical Society: Washington, DC. 2-12.

87. Thakur BR, Singh RK, Handa AK, Rao MA. *Chemistry and uses of pectin — A review*, Crit Rev Food Sci Nutr 1997; 37(1): 47-73.

88. Ducheňe D, Touchard F, Peppas NA. *Pharmaceutical and medical aspects of bioadhesive systems for drug administration*, Drug Dev Ind Pharm 1988; 14(2-3): 283-318.

89. Schmidgall J, Hensel A. *Bioadhesive properties of polygalacturonides against colonic epithelial membranes*, Int J Biol Macromol 2002; 30(5): 217-225.

90. Hagesaether E, Sande SA. *In vitro measurements of mucoadhesive properties of six types of pectin*, Drug Dev Ind Pharm 2007; 33(4): 417-425.

91. Hagesaether E, Bye R, Sande SA. *Ex vivo mucoadhesion of different zinc-pectinate hydrogel beads*, Int J Pharm 2008; 347(1-2): 9-15.

92. Sharma R, Ahuja M, Kaur H. *Thiolated pectin nanoparticles: Preparation, characterization and ex vivo corneal permeation study*, Carbohydr Polym 2012; 87(2): 1606-1610.

93. Cheng K, Lim LY. *Insulin-loaded calcium pectinate nanoparticles: effects of pectin molecular weight and formulation pH*, Drug Dev Ind Pharm 2004; 30(4): 359-67.

94. Smistad G, Bøyum S, Alund SJ, Samuelsen ABC, Hiorth M. *The potential of pectin as a stabilizer for liposomal drug delivery systems*, Carbohydr Polym 2012; 90(3): 1337-1344.

95. Racape E, Thibault JF, Reitsma JCE, Pilnik W. *Properties of amidated pectins. II. Polyelectrolyte behavior and calcium binding of amidated pectins and amidated pectic acids*, Biopolymers 1989; 28(8): 1435-1448.

96. Wåler SM. *The effect of zinc-containing chewing gum on volatile sulfur-containing compounds in the oral cavity*, Acta Odontol Scand 1997; 55(3): 198-200.

97. Schärtl W, *Light scattering from polymer solutions and nanoparticle dispersions*. 1st ed. 2007, Springer-Verlag: Berlin/Heidelberg.

98. Klemetsrud T, Jonassen H, Hiorth M, Kjøniksen A-L, Smistad G. *Studies on pectin-coated liposomes and their interaction with mucin*, Colloids Surf B Biointerfaces 2013; 103(0): 158-165.

99. Freitas C, Müller RH. *Effect of light and temperature on zeta potential and physical stability in solid lipid nanoparticle (SLN™) dispersions*, Int J Pharm 1998; 168(2): 221-229.

100. Ney P, *Zeta-Potentiale und Flotierbarkeit von Mineralen*. 1st ed. 1973, Springer: Wien.

101. Schwarz C, Mehnert W, Lucks JS, Müller RH. *Solid lipid nanoparticles (SLN) for controlled drug delivery. I. Production, characterization and sterilization*, J Control Release 1994; 30(1): 83-96.

102. Tsaih ML, Chen RH. *Effect of molecular weight and urea on the conformation of chitosan molecules in dilute solutions*, Int J Biol Macromol 1997; 20(3): 233-240.

103. Dobrynin AV, Rubinstein M. *Theory of polyelectrolytes in solutions and at surfaces*, Prog Polym Sci 2005; 30(11): 1049-1118.

104. Chen W, Hsu C, Huang J, Tsai M, Chen R. *Effect of the ionic strength of the media on the aggregation behaviors of high molecule weight chitosan*, J Polym Res 2011: 1-11.

105. Al-Manasir N, Kjøniksen A-L, Nyström B. *Preparation and characterization of cross-linked polymeric nanoparticles for enhanced oil recovery applications*, J Appl Polym Sci 2009; 113(3): 1916-1924.

106. Sundararaj U, Macosko C. *Drop breakup and coalescence in polymer blends: the effects of concentration and compatibilization*, Macromolecules 1995; 28(8): 2647-2657.

107. de Campos AM, Diebold Y, Carvalho ELS, Sanchez A, Alonso MJ. *Chitosan nanoparticles as new ocular drug delivery systems: in vitro stability, in vivo fate, and cellular toxicity*, Pharm Res 2004; 21: 803-810.

108. Keawchaoon L, Yoksan R. *Preparation, characterization and in vitro release study of carvacrol-loaded chitosan nanoparticles*, Colloids Surf B Biointerfaces 2011; 84: 163-171.

109. Tanaka H. *Appearance of a moving droplet phase and unusual networklike or spongelike patterns in a phase-separating polymer solution with a double-well-shaped phase diagram*, Macromolecules 1992; 25: 6377-6380.

110. Tanaka H. *Unusual phase separation in a polymer solution caused by asymmetric molecular dynamics*, Phys Rev Lett 1993; 71(19): 3158-3161.

111. Huang Y, Lapitsky Y. *Salt-assisted mechanistic analysis of chitosan/tripolyphosphate micro- and nanogel formation*, Biomacromolecules 2012; 13(11): 3868-3876.

112. Su X, Jessop PG, Cunningham MF. *Surfactant-free polymerization forming switchable latexes that can be aggregated and redispersed by $CO_2$ removal and then readdition*, Macromolecules 2012; 45(2): 666-670.

113. Sriamornsak P, Wattanakorn N. *Rheological synergy in aqueous mixtures of pectin and mucin*, Carbohydr Polym 2008; 74(3): 474-481.

114. Sriamornsak P, Wattanakorn N, Takeuchi H. *Study on the mucoadhesion mechanism of pectin by atomic force microscopy and mucin-particle method*, Carbohydr Polym 2010; 79(1): 54-59.

115. Thirawong N, Kennedy RA, Sriamornsak P. *Viscometric study of pectin–mucin interaction and its mucoadhesive bond strength*, Carbohydr Polym 2008; 71(2): 170-179.

116. Sogias IA, Williams AC, Khutoryanskiy VV. *Why is chitosan mucoadhesive?*, Biomacromolecules 2008; 9(7): 1837-1842.

117. Jonassen H, Kjøniksen A-L. *Optical-scattering method for the determination of the local polymer concentration inside nanoparticles*, Phys Rev E 2011; 84(2): 022401.

118. Trinh LTT, Lambermont-Thijs HML, Schubert US, Hoogenboom R, Kjøniksen A-L. *Thermoresponsive poly(2-oxazoline) block copolymers exhibiting two cloud points: complex multistep assembly behavior*, Macromolecules 2012; 45(10): 4337-4345.

119. Dashtimoghadam E, Mirzadeh H, Taromi FA, Nyström B. *Microfluidic self-assembly of polymeric nanoparticles with tunable compactness for controlled drug delivery*, Polymer 2013; 54(18): 4972-4979.

120. Collnot E-M, Ali H, Lehr C-M. *Nano- and microparticulate drug carriers for targeting of the inflamed intestinal mucosa*, J Control Release 2012; 161(2): 235-246.

121. Pilcer G, Amighi K. *Formulation strategy and use of excipients in pulmonary drug delivery*, Int J Pharm 2010; 392(1–2): 1-19.

122. Vanić Ž, Škalko-Basnet N. *Nanopharmaceuticals for improved topical vaginal therapy: Can they deliver?*, Eur J Pharm Sci 2013; 50(1): 29-41.

123. Wen MM. *Olfactory targeting through intranasal delivery of biopharmaceutical drugs to the brain: current development*, Discov Med 2011; 11(61): 497-503.

124. Sudhakar Y, Kuotsu K, Bandyopadhyay AK. *Buccal bioadhesive drug delivery -- A promising option for orally less efficient drugs*, J Control Release 2006; 114(1): 15-40.

# I

# Optical-scattering method for the determination of the local polymer concentration inside nanoparticles

Helene Jonassen[1] and Anna-Lena Kjøniksen[1,2,*]

[1]*Department of Pharmacy, School of Pharmacy, University of Oslo, Post Office Box 1068, Blindern, N-0316 Oslo, Norway*

[2]*Department of Chemistry, University of Oslo, Post Office Box 1033, Blindern, N-0315 Oslo, Norway*

(Received 26 April 2011; published 8 August 2011)

We have developed a method based on the Mie theory for determining the local polymer concentration inside spherical nanoparticles, thereby obtaining vital information about whether the particles are swelling in the solvent or if they are contracted into a more compact structure. In addition, this method can be used to calculate the number density of the particles, the molecular weight of the particles, and (if $M_n$ of the polymer is known) the aggregation number. The calculations are based on the relationship between the size of the nanoparticles and the turbidity of the sample.

DOI: 10.1103/PhysRevE.84.022401 PACS number(s): 83.80.Hj, 78.67.Sc, 61.46.Df, 82.35.Lr

Polymer nanoparticles have been the subject of a vast number of studies, both to gain a better fundamental understanding of their properties [1] and to develop numerous interesting applications for them [2]. Polymer nanoparticles can be made either by covalently cross-linking polymers into permanent particles, sometimes referred to as nanogels, or by assembling several polymer units together by physical interactions such as hydrogen bonds, electrostatic forces, or hydrophobic associations. The size of the particles is dependent on the amount of polymer they contain and on how much they swell in the solvent they are suspended in. However, the attractive forces that cause the particles to contract will often induce aggregation between the nanoparticles. The competition between intra- and interparticle associations is often observed for stimuli-responsive systems [1,3–7] where the attractive forces between the polymer chains can be turned on and off by changes in external parameters such as temperature, solvent salinity, or pH. This can make it difficult to interpret changes in particle size, since an increase in size can be caused by either swelling or aggregation, and constant size can actually be the result of a cancelation between contraction and aggregation of the particles [6]. In order to gain a proper understanding of nanoparticular systems, it is important to characterize the degree of swelling (i.e., the local polymer concentration inside the nanoparticles).

In addition to being helpful in the interpretation of changes in particle size, the local polymer concentration inside the nanoparticles is in itself important for various applications. Polymer nanoparticles are of interest for controlled drug delivery [8], and one of the factors that affect the release rate of drugs from nanoparticle suspensions is the degree of swelling of the particles, as the more open structure of swollen nanoparticles has been observed to increase the drug release rate from the particles [9–11]. Polymer nanoparticles also can be used to make temperature-responsive polymeric photosensitizers, which have been found to be dependent on the hydration and dehydration of the nanoparticles [12,13], that is, the local polymer concentration inside the nanoparticles. Another application of polymer nanoparticles is water purification, and in connection with this it has been suggested that the degree of particle swelling can control the uptake and release of Pb(II) ions [14].

The aggregation of polymer nanoparticles into larger aggregates is also governed by the local polymer concentration inside the nanoparticles [1,15–17]. Aggregate formation is dependent on the contact time between the particles when they collide ($\tau_c$) and the time needed to establish a permanent chain entanglement between two approaching particles ($\tau_e$). When $\tau_c \ll \tau_e$, aggregate formation is suppressed since the colliding particles do not have time to stick together, and the particles behave as elastic bodies on the collision time scale. Tanaka [15,16] showed that $\tau_c$ and $\tau_e$ can be estimated by

$$\frac{r_0}{\langle \upsilon \rangle} < \tau_c < \frac{r_0^2}{D} \quad \text{and} \quad \tau_e \sim \frac{a_m^2 N_m^3 \phi_{\mathrm{NP}}^{3/2}}{D_m} \tag{1}$$

where $r_0$ is the interaction range between the particles, $\langle \upsilon \rangle$ is the thermal velocity magnitude ($\langle \upsilon \rangle \sim (kT/m_p)^{1/2}$, where $k$ is Boltzmann's constant, $T$ is the absolute temperature, $m_p$ is the mass of the particle), $D$ is the diffusion coefficient of the particles ($D = \frac{kT}{6\pi\eta_0 R}$, where $\eta_0$ is the viscosity of the solvent and $R$ is the radius of the particle), $a_m$ is the length of a unit monomer, $N_m$ is the number of monomers, $\varphi_{\mathrm{NP}}$ is the volume fraction of polymer inside the particles, and $D_m$ is the diffusion coefficient of the monomer. Accordingly, $\tau_e$ increases with the aggregation number and with the volume fraction of polymer inside the particles, and aggregation is therefore suppressed when the local polymer concentration inside the nanoparticles is high enough.

The degree of swelling of nanoparticles has been determined by separating the nanoparticles from the solvent by filtration and comparing the weight of the swollen nanoparticles with their dry mass [9]. However, separation of small nanoparticles from the solvent can be experimentally difficult, and this method is not very well suited for nanoparticles that are sensitive to changes in temperature or concentration. The local polymer concentration inside nanoparticles can also be determined by comparing their size with the molecular weight

*a.l.kjoniksen@kjemi.uio.no

 

of the particles [1]. Unfortunately, determining the molecular weight of nanoparticles can be experimentally challenging. The aggregation number of the particles is often concentration dependent, which excludes the use of separation methods which will dilute the system system (such as gel permeation chromatography, size exclusion chromatography or asymmetric flow field-flow fractionation), and even the determination of the molecular weight by a traditional Zimm plot, for which a concentration series is needed. For very low polymer concentrations, the molecular weight can be estimated from a single polymer concentration from either a Zimm plot for small particles or a Guinier plot for large particles [1], but the limitation to very low concentrations restricts the usefulness of these techniques. A method for determining the local polymer concentration inside nanoparticles from experiments that can easily be conducted on nanoparticle suspensions at various temperatures and polymer concentrations is therefore needed. In this paper, we illustrate how the local polymer concentration inside spherical nanoparticles, as well as their number density, molecular weight, and aggregation number, can be determined from the size of the nanoparticles and the turbidity of the nanoparticle suspension.

The turbidity ($\tau$) of a sample containing nanoparticles can be expressed by Lambert-Beer's law:

$$\tau = -\frac{1}{L}\ln\left(\frac{I}{I_0}\right), \tag{2}$$

where $L$ is the thickness of the cell, $I$ is the light transmitted through the sample, and $I_0$ is the light transmitted through the solvent. The turbidity of the sample is dependent on the number density of particles $N$ (number of particles per unit volume), the radius $R$ of the particles, and the difference in refractive index between the particles and the surrounding media [18]:

$$\tau = N\pi R^2 Q_{\text{ext}}, \tag{3}$$

where $Q_{\text{ext}}$ is the Mie extinction efficiency. For spherical particles that do not absorb light at the considered wavelength ($\lambda$), the Mie extinction efficiency can be expressed as [19,20]

$$Q_{\text{ext}} = 2\left[1 - \frac{2}{\rho}\left(\sin\rho - \frac{1}{\rho}(1-\cos\rho)\right)\right], \tag{4}$$

where $\rho = \frac{4\pi R(m-1)}{\lambda}$, and $m = \frac{n_{\text{NP}}}{n_0}$ is the ratio between the refractive index of the particle ($n_{\text{NP}}$) and the refractive index of the solvent ($n_0$). The refractive index of the particle can be expressed in terms of the refractive index increment of the polymer ($dn/dc$) by $n_{\text{NP}} = n_0 + (dn/dc)\,c_{\text{NP}}$, where $c_{\text{NP}}$ is the local polymer concentration inside a nanoparticle. This gives us

$$\rho = \frac{4\pi R\,(dn/dc)\,c_{\text{NP}}}{\lambda n_0} = w c_{\text{NP}}, \tag{5}$$

where $w = \frac{4\pi R(dn/dc)}{\lambda n_0}$.

For a sample with a total volume $V_t$, the total mass of polymer in the nanoparticles can be expressed as $m_t = N_{\text{NP}} m_{\text{NP}}$, where $m_{\text{NP}}$ is the mass of polymer in a single nanoparticle and $N_{\text{NP}} = N V_t$ is the total number of particles in the sample. The total polymer concentration can be expressed as $c_t = \frac{m_t}{V_t}$, and the local polymer concentration inside a single nanoparticle with a volume $V_{\text{NP}}$ is

$$c_{\text{NP}} = \frac{m_{\text{NP}}}{V_{\text{NP}}} = \frac{3 m_{\text{NP}}}{4\pi R^3}. \tag{6}$$

Accordingly, the number density of particles can be expressed as

$$N = \frac{3c_t}{4 c_{\text{NP}} \pi R^3}. \tag{7}$$

By combining Eqs. (3), (4), (5), and (7), we can now express the turbidity as

$$\tau = \frac{3c_t}{2c_{\text{NP}}R}\left(1 - \frac{2}{w c_{\text{NP}}}\left\{\sin(w c_{\text{NP}}) - \frac{1}{w c_{\text{NP}}}[1-\cos(w c_{\text{NP}})]\right\}\right). \tag{8}$$

As can be seen from Eq. (8), the turbidity is now expressed as a function of $c_{\text{NP}}$. For a sample containing spherical nanoparticles with a relatively narrow size distribution, we can now determine the local polymer concentration inside the nanoparticles.

Chitosan is a nontoxic biopolymer with promising properties for various drug delivery purposes [21]. It can be crosslinked by tripolyphosphate (TPP), which is a polyanion that interacts electrostatically with the positively charged chitosan [21]. By adding TPP to dilute solutions of chitosan, we can thereby form physically cross-linked nanoparticles. We have measured the hydrodynamic radius of chitosan (Protasan; chitosan chloride) nanoparticles cross-linked by TPP in the presence of 0.1 M NaCl at different cross-linker concentrations by dynamic light scattering (DLS). The hydrodynamic radius of the nanoparticles is determined from DLS measurements as described previously [5]. As can be seen from Fig. 1, when the cross-linker concentration is increased, the radius goes through a slight maximum before it decreases markedly at high cross-linking densities.

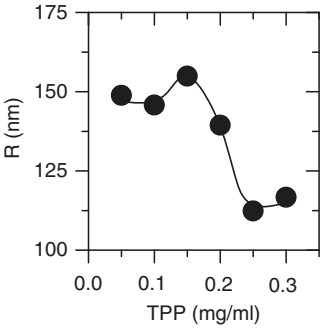


FIG. 1. Hydrodynamic radius of chitosan nanoparticles determined by DLS as a function of cross-linker concentration. The errors are of approximately the same size as the symbols, and the line is only a guide for the eye.

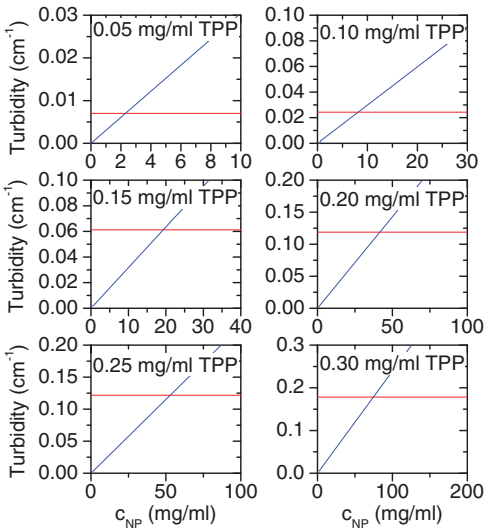


FIG. 2. (Color online) The turbidity of suspensions of chitosan nanoparticles at the indicated cross-linker concentrations as a function of the local polymer concentration inside the nanoparticles calculated from Eq. (8) using the sizes determined by DLS are represented by the sloping (blue) lines. The horizontal (red) lines indicate the turbidities determined from the transmittance data from Eq. (2).

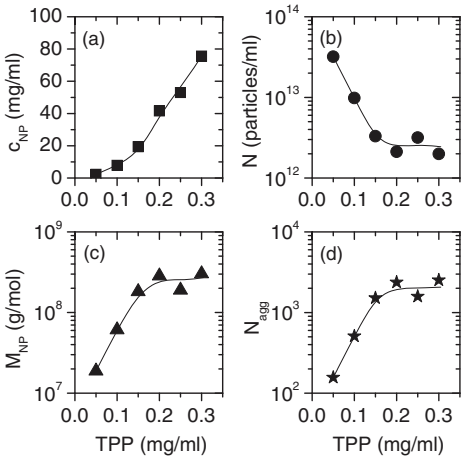


FIG. 3. (a) The local polymer concentration in the chitosan nanoparticles, (b) the number density of nanoparticles, (c) the molecular weight of the nanoparticles, and (d) the aggregation number of chitosan in the nanoparticles as a function of the cross-linker concentration. The lines are only guides for the eye.

Considering both the relatively high cross-linker concentrations used and that the presence of NaCl in the sample will promote aggregation, it is reasonable to assume that practically all chitosan is in the form of nanoparticles and very little polymer is left as free polymer chains in the solution. This assumption is corroborated by the measured correlation functions, which exhibit only one relaxation mode with a narrow size distribution. We therefore can assume that the total polymer concentration in the sample is in the form of nanoparticles, giving us $c_t = 1.0$ mg/ml, which equals the total chitosan concentration in the samples. We have measured the refractive index increment of chitosan in 0.1 M NaCl to be $dn/dc = 0.157$ g/ml, and the refractive index of the solvent is $n_0 = 1.3337$. The transmittance of the samples was measured on a spectrophotometer at a wavelength of 633 nm, and the turbidity was calculated from Eq. (2).

In Fig. 2, the turbidity of each sample is plotted as a function of $c_{NP}$ from Eq. (8), using the hydrodynamic radii measured by DLS. The horizontal lines indicate the turbidities calculated from Eq. (2). The local polymer concentration inside the nanoparticles can be determined from the intercept between the two lines. Figure 3(a) illustrates how $c_{NP}$ varies with the cross-linker density, and as expected a higher cross-linker concentration increases the local polymer concentration inside the particles as enhanced intraparticle cross links causes the particles to contract.

Having determined $c_{NP}$, we can now calculate the number density of the particles by using Eq. (7). From Fig. 3(b) we can see that the number density decreases with increasing cross-linker concentration, indicating that the cross-linking process is not only establishing intraparticle cross links within pre-existing polymer aggregates, but in addition interparticle cross links are binding several aggregates together, thereby reducing the total number of particles in the sample. From Eq. (6), we can see that $m_{NP} = \frac{4}{3}\pi R^3 c_{NP}$, which gives us the molecular weight of the particles as

$$M_{NP} = \tfrac{4}{3}\pi R^3 c_{NP} N_A, \tag{9}$$

where $N_A$ is Avogadro's number. We can now determine the aggregation number from

$$N_{agg} = \frac{M_{NP}}{M_n}, \tag{10}$$

where $M_n$ is the number average molecular weight of the polymer ($1.2 \times 10^5$). As can be seen from Figs. 3(c) and 3(d), both the molecular weight of the particles and the aggregation number increase as more cross linker is added to the sample, again illustrating that higher cross-linking densities enhances interparticle aggregation. Comparing the various characteristics of the particles, we can see that at low cross-linker concentrations, the contraction of the particles is relatively modest [Fig. 3(a)] while the aggregation number rises markedly [Fig. 3(d)]. This causes the observed increase in size (Fig. 1). At high cross-linker concentrations, the aggregation number of the nanoparticles is nearly constant, while the local concentration inside the particles rises markedly. At this stage both $N_{agg}$ and $c_{NP}$ are high, and we can assume that $\tau_c \ll \tau_e$. Further aggregation is therefore suppressed, and the cross-linking process is mainly taking place inside the existing particles, causing them to contract into smaller particles (Fig. 1).

In summary, we have developed a method for determining the local polymer concentration inside polymer nanoparticles. The method has been tested on chitosan nanoparticles

crosslinked by TPP and shows that as expected $c_{NP}$ increases with the cross-linking density. We have also been able to determine the number density of particles in the solution, the molecular weight of the particles, and the aggregation number of chitosan in the nanoparticles. The obtained results are in agreement with what one would expect for the considered nanoparticles.

We gratefully acknowledge financial support from the Norwegian Research Council for Project 190403.

[1] G. Zhang and C. Wu, Adv. Polym. Sci. **195**, 101 (2006).
[2] M. Motornov, Y. Roiter, I. Tokarev, and S. Minko, Prog. Polym. Sci. **35**, 174 (2010).
[3] C. Gao, B. Chen, and H. Möhwald, Colloid. Surf. A: Physicochem. Eng. Asp. **272**, 203 (2006).
[4] K. Skrabania, J. Kristen, A. Laschewsky, Ö. Akdemir, A. Hoth, and J.-F. Lutz, Langmuir **23**, 84 (2007).
[5] N. Al-Manasir, K. Zhu, A.-L. Kjøniksen, K. D. Knudsen, G. Karlsson, and B. Nyström, J. Phys. Chem. B **113**, 11115 (2009).
[6] J. Madsen, S. P. Armes, K. Bertal, S. MacNeil, and A. L. Lewis, Biomacromolecules **10**, 1875 (2009)
[7] J. Zhao, G. Zhang, and S. Pispas, J. Polym. Sci. A: Polym. Chem. **48**, 2320 (2010).
[8] A. K. Bajpai, S. K. Shukla, S. Bhanu, and S. Kankane, Prog. Polym. Sci. **33**, 1088 (2008).
[9] R. Chouhan and A. K. Bajpai, Nanomedicine: NBM **6**, 453 (2010).
[10] S. Kim, J.-H. Kim, and D. Kim, J. Colloid Interface Sci. **356**, 100 (2011).
[11] L. Keawchaoon and R. Yoksan, Colloid. Surf. B: Biointerfaces **84**, 163 (2011).
[12] H. Koizumi, Y. Shiraishi, S. Tojo, M. Fujitsuka, T. Majima, and T. Hirai, J. Am. Chem. Soc. **128**, 8751 (2006).
[13] Y. Shiraishi, Y. Kimata, H. Koizumi, and T. Hirai, Langmuir **24**, 9832 (2008).
[14] G. E. Morris, B. Vincent, and M. J. Snowden, J. Colloid Interface Sci. **190**, 198 (1997).
[15] H. Tanaka, Macromolecules **25**, 6377 (1992).
[16] H. Tanaka, Phys. Rev. Lett. **71**, 3158 (1993).
[17] S. Piçarra and J. M. G. Martinho, Macromolecules **34**, 53 (2001).
[18] M. D. Lechner, J. Serb. Chem. Soc. **70**, 361 (2005).
[19] T. W. Chen, J. Mod. Optic. **35**, 743 (1988).
[20] X. Sun, H. Tang, and G. Yuan, J. Quantum. Spectrosc. Radiat. Transf. **109**, 89 (2008).
[21] M. Dash, F. Chiellini, R. M. Ottenbrite, and E. Chiellini, Prog. Polym. Sci. **36**, 981 (2011).